RAA 2018 Vol. **18** No. **6**, 68(22pp) doi: 10.1088/1674–4527/18/6/68

http://www.raa-journal.org *http://iopscience.iop.org/raa*

Research in Astronomy and Astrophysics

Cataclysmic variables based on the stellar spectral survey LAMOST DR3

Xianming L. Han[1,2,3], Li-Yun Zhang[1,3], Jian-Rong Shi[4], Qing-Feng Pi[5], Hong-Peng Lu[1,3], Li-Bo Zhao[1,3], Rachel K. Terheide[2] and Lin-Yang Jiang[1,3]

[1] College of Physics/Department of Physics and Astronomy & Guizhou Provincial Key Laboratory of Public Big Data, Guizhou University, Guiyang 550025, China; *liy_zhang@hotmail.com*

[2] Dept. of Physics and Astronomy, Butler University, Indianapolis, IN 46208, USA

[3] Key Laboratory for the Structure and Evolution of Celestial Objects, Chinese Academy of Sciences, Kunming 650011, China

[4] National Astronomical Observatories, Chinese Academy of Sciences, Beijing 100101, China

[5] Department of Astronomy, Beijing Normal University, Beijing 100875, China

Received 2017 November 30; accepted 2018 March 12

Abstract Big data in the form of stellar spectra from the spectroscopic survey associated with the Large Sky Area Multi-object Fiber Spectroscopic Telescope (LAMOST) are important for studying properties of cataclysmic variables (CVs). By cross matching the catalogs of CVs compiled with LAMOST DR3, acquired from October 2011 to July 2015, we obtained the first spectroscopic catalog for CVs observed by LAMOST with high signal to noise ratio, above 8. By integrating line profiles, their equivalent widths (EWs) of the Hα, Hβ, Hγ and Hδ, as well as He I 5876 and 6678 Å lines, were calculated. There were 74 stellar spectra from 48 known CVs and three spectra from three new CV candidates. At the same time, we also collected their previously published EWs. Thirty-three objects had repeated spectra and 30 stars showed spectral variability in the Hα line. Moreover, we carried out photometric follow-up studies for five CVs (UU Aqr, TT Tri, PX And, BP Lyn and RW Tri). We obtained nine new light curves and revised their linear ephemerides. For RW Tri, there is a possible oscillation with an amplitude of 0.0031(2) days and a period of 47.6 ± 0.4 years, which might be caused by a third body (brown dwarf) or magnetic activity cycle.

Key words: stars: cataclysmic variables — stars: spectroscopic — stars: variable

1 INTRODUCTION

Cataclysmic variable (CV) stars are compact binary stars consisting of a white dwarf, with temperatures ranging from 10 000–50 000 K, accreting from the Roche lobe of its companion star which is usually a low mass-main sequence star with temperature of 3000–5000 K (Sion 1986; Warner 1995; etc). They can be observed in optical, ultraviolet, extreme ultraviolet, infrared and X-ray wavelengths, including wavelengths accessible by the *International Ultraviolet Explorer*, to understand their properties and evolutional trends (Giovannelli 2008; Liu et al. 1999; etc).

Downes et al. (2001) published an online updated catalog and atlas of about 1600 CVs and 229 non-CVs, that includes their classifications, orbital periods, magnitudes and spectral information (776 objects show quiescent spectra, 191 objects present outburst spectra and 632 objects have no spectra). Using the Sloan Digital Sky Survey (SDSS) (e.g. York et al. 2000), Szkody et al. (2002) identified 22 CVs, including 19 new discoveries and three previously known systems. They also carried out follow-up observations to determine the orbital periods of the three new objects. Afterwards, they also identified many CVs through SDSS spectra and determined their spectral properties and orbital periods by follow-up spectroscopic and photometric observations (Szkody et al. 2002, 2003, 2004, 2005, 2006, 2007, 2009). Recently, they published a complete catalog of 285 CVs with spectra in an online table of all known CVs from both photometric and spectroscopic observations

(Szkody et al. 2011). The Catalina Real-time Transient Survey (CRTS) discovered 1043 CV candidates and published the largest sample of CVs from a single survey in six years (Breedt et al. 2014; Drake et al. 2014). They also provided spectroscopic identifications of 85 systems and discovered that 53 percent of the CVs they analyzed had variable amplitudes (Breedt et al. 2014; Drake et al. 2014; etc).

CVs have been studied by many groups to determine their orbital period (Dillon et al. 2008; Southworth et al. 2006; Kato et al. 2009; etc), orbital period variation and related physical mechanisms (Qian et al. 2010; Dai et al. 2013) by time series photometry. By conducting photometric and spectroscopic observations of CV candidates discovered from SDSS and CRTS, Szkody (2014) confirmed their types (dwarf novae, nova-like cases or polars), and determined their orbital periods and spectroscopic properties (outburst or quiescence). Through a series of high-speed photometric observations of many faint CVs selected from the SDSS and CRTS, Woudt et al. (2012) also determined their orbital periods. Southworth et al. (2015) reported the discovery of eclipsing CVs and determined the parameters of the system using high-speed photometry. Furthermore, they investigated the orbital period distribution within the SDSS samples and for all CVs with known orbital periods (Southworth et al. 2006, 2015).

Built by the Chinese Academy of Sciences, the Large Sky Area Multi-Object Fiber Spectroscopic Telescope, (LAMOST, also known as the Guo Shou Jing Telescope) has become an important scientific project for spectral surveys. Wei et al. (2013, 2014) developed the LAMOST spectral analysis pipeline to classify different subclasses by matching with template spectra. This approach has proven to be an effective and efficient novel method for identifying CVs from optical spectra through the support vector machine technique combined with principal component analysis. They identified 11 previously known CVs (Wei et al. 2013, 2014). Jiang et al. (2013) also developed an effective data-mining method to find CVs from LAMOST spectra, and identified 10 previously known CVs and two new CV candidates. The LAMOST project has published over four million spectra, which is a useful resource for examining their properties and searching for new CV candidates.

In this paper, we present known and unknown CVs observed by the LAMOST spectral survey, and obtain their equivalent widths (EWs) of several spectral lines, including Hα, Hβ, Hγ, Hδ and He I 5876 and 6678 Å. We also present light curves from our photometric follow-up observations of five CVs (UU Aqr, TT Tri, PX And, BP Lyn and RW Tri), and our new primary minima and their revised linear ephemerides.

2 DATA

LAMOST is a Chinese optical telescope with a field of view of about five square degrees and an effective aperture of about 4 meters (Wang et al. 1996, Cui et al. 2012). There are 16 low resolution spectrographs with a double-beam full Schmidt design and volume phase holographic gratings, which can simultaneously acquire spectra of about 4000 celestial objects via fibers located in its field of view (Cui et al. 2012; Wang et al. 1996). The resolution is about 1800 and the wavelength region is about 3700–9000 Å. The exposure time for a single CCD observation is 30 min and we combine three continuous exposures for a total effective exposure time of about 1.5 hours. The red wavelength is calibrated by an NeAr lamp and the blue wavelength is calibrated by an HgCd lamp. The observed spectra were not flux-calibrated by matching the selected standard flux stars. LAMOST has published over 4 million stellar spectra in LAMOST Data Release 3 (DR3) (*http://dr3.lamost.org/*) from the survey carried out from October 2011 – July 2015 (Luo et al. 2015). The stellar spectra were from the systematic spectroscopic surveys of a large number stars in the Galactic disk, the defining structure and halo (e.g., Chen et al. 2012; Deng et al. 2012, Liu et al. 2015). We downloaded these spectra from LAMOST's official website. The associated CCD data were reduced by the LAMOST 2D pipeline software (Luo et al. 2012, 2015), which includes bias and dark subtraction, flat field correction, spectral extraction, sky subtraction and wavelength calibration (Luo et al. 2012, 2015). There are two separate channels and spectrographs. The wavelength region of the blue channel is about 370–590 nm and the wavelength region of the red channel is about 570–900 nm. The LAMOST group combined two parts of the spectra from the red and blue spectrographs into a single spectrum for each target. For some LAMOST spectra, there is a bad region (missing) near 6000 Å because of the process involved in combining the two parts of LAMOST spectra.

We cross-matched the updated catalog of CVs (Downes et al. 2001), 1043 CV candidates identified by CRTS (Breedt et al. 2014) and 285 CVs identified from SDSS (Szkody et al. 2011) with stellar spectra from LAMOST DR3. Identifying new CVs will give us a better understanding of the total spatial density of all types of CVs (Szkody 2015) and the physical properties and evolutions of CVs (Giovannelli 2008), such as physical parameters, mass transfer process, spectral line emission properties and so on. Therefore, we also collected the new CV candidates detected by the LAMOST survey through matching with template spectra developed by Wei et al. (2013, 2014). The methods of identifying CVs from optical spectra are described in detail in their papers (Jiang et al. 2013; Wei et al. 2013, 2014). Moreover, we identified new CVs from optical spectra using the support vector machine technique combined with principal component analysis. After excluding most non-CVs using these two methods, we identified CVs manually or by a template-matching algorithm using the spectra of dwarf novae at quiescence, magnetic CVs and nova-like variables with obvious emission lines, and so on (Jiang et al. 2013; etc). We chose the CVs or new CV candidates observed in the LAMOST spectral survey with signal to noise ratio (S/N) above 8 in the R band. We listed these parameters in Table 1, where the first column indicates an object's CV status (cv01 means known CV, newcv# means it is a new CV candidate, and noncv means it was identified as not a CV in the previous CV catalog published by Downes et al. (2001)), LAMOST name in the second column, other name in the third column, information about whether a spectrum is newly observed or not is listed in the fourth column ("Y" means that the spectrum is first observed by LAMOST, while "N" means it is not.), observation date is in the 5th column, magnitudes of $ugrizJHK$ are provided from the 6th to 13th columns respectively, their S/Ns) in $ugriz$ from 14th to 18th columns respectively, and references in the last column. We obtained 92 LAMOST spectra for 62 objects: 74 spectra of 48 known CVs, three spectra of three new CV candidates and 15 spectra of 11 non-CVs in the updated CV catalog (Downes et al. 2001). This is the first time that the spectra of six known CVs and three newly identified CVs candidates were obtained.

3 ANALYSES OF LAMOST SPECTRA OF CVS

In this section, we will discuss the spectroscopic properties of CVs, and present our photometric follow-up observations of several CVs with their revised linear ephemerides.

3.1 Spectroscopic Properties of CVs

From LAMOST DR3, we identified 74 stellar spectra associated with 48 known CVs, and three spectra representing three new CV candidates, as well as 15 spectra corresponding to 11 objects classified as non-cv objects in the previous CV catalog. We plot several sample CVs with only one LAMOST spectrum in Figure 1. The fluxes associated with our observed spectra are not calibrated using standard stars. The left panels show the observed spectra, and the vertical axis represents the raw CCD electron counts. In the right panels, we plot the normalized spectra, where the signals are normalized to their continuum by a 5 or 6 order polynomial fit using the continuum package in the IRAF software[1]. We measured the EWs by integrating over the emission profile using the Splot package in the IRAF program. The methods for calculating the EWs and their uncertainties are similar to those of Zhang & Gu (2008).

The results are presented in Table 2, which includes the star number (first column), LAMOST name (second column), Heliocentric Julian Date (HJD) (third column), EWs of Hα (fourth column), variation of Hα EWs (fifth column), and EWs of Hβ, Hγ, Hδ and He I 5876 Å and 6678 Å lines (6th–10th columns). We note that some of the LAMOST spectra have a bad region in the red wavelength region at about 8500 Å. Furthermore, we searched the literature for existing EWs in Hα and Hβ in the 11th and 12th columns, and list their references in the last column of Table 2. We also identified 33 objects with repeated observations. We further determined spectral EW variability by the difference in the maximum and minimum EWs in the Hα line: When this difference is larger than three times its corresponding error (Zhang et al. 2016, 2017), we consider the object's spectrum to be variable. Among these 33 objects, 30 CVs showed spectral variations, while three objects showed no spectral variation. We plotted some repeated LAMOST spectra and normalized them to their continuum in Figure 2.

As can be seen from Figures 1 and 2, there are strong He II 4686 Å emission lines for some of them (LAMOST J003005.80+261726.3, LAMOST J053159.11+302644.9, T Aur, V647 Aur, V418 Gem, DW CNc, BH Lyn, ...). For AM Her, its spectrum shows characteristics of being a double star because two parts of the continuum in the red and blue wavelengths are higher in the middle region. The large amount of LAMOST data was very useful for searching for new CV candidates. We found three new CV candidates and list them in Tables 1 and 2, and plot their observed (left panel) and normalized spectra (right panel) in Figure 3.

[1] IRAF is distributed by the National Optical Astronomy Observatories, which are operated by the Association of Universities for Research in Astronomy, Inc., under cooperative agreement with the National Science Foundation.

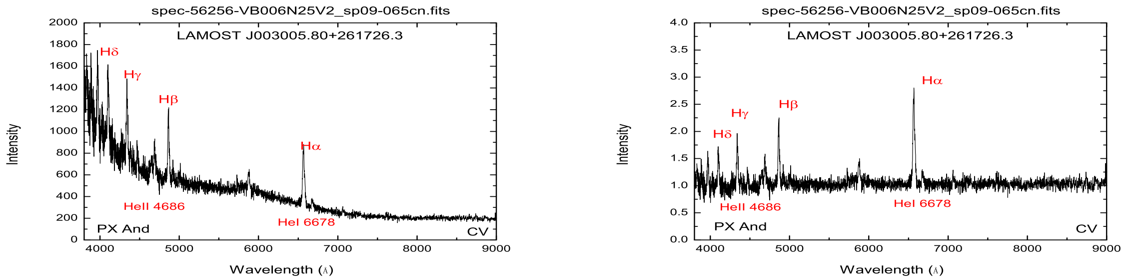

(a) CV:LAMOST J003005.80+261726.3

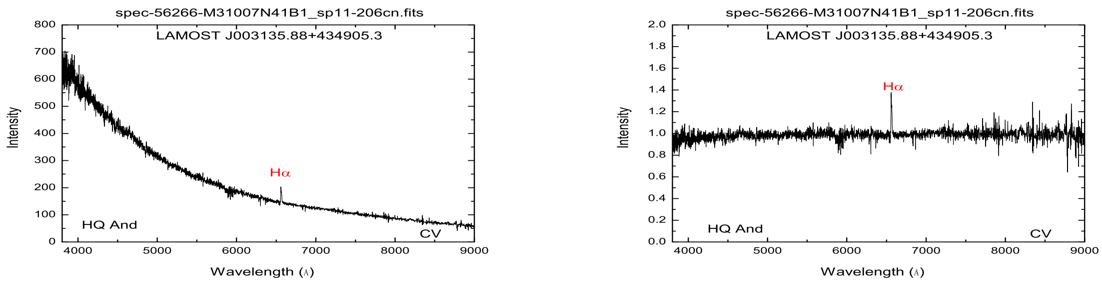

(b) CV: LAMOST J003135.88+434905.3

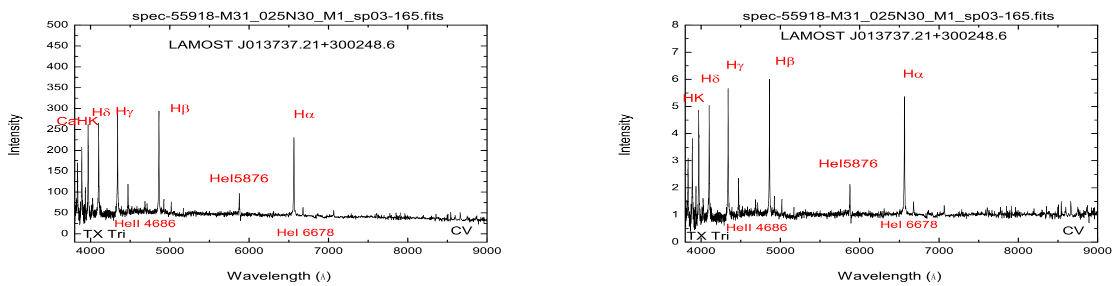

(c) CV: LAMOST J013737.21+300248.6

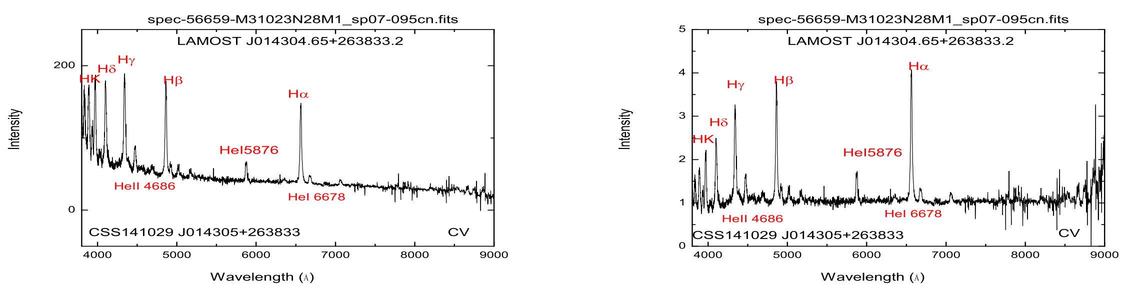

(d) CV: LAMOST J014304.65+263833.2

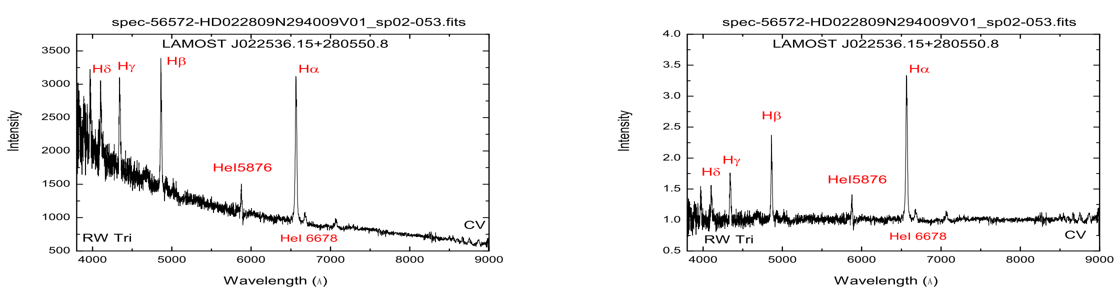

(e) CV: LAMOST J022536.15+280550.8

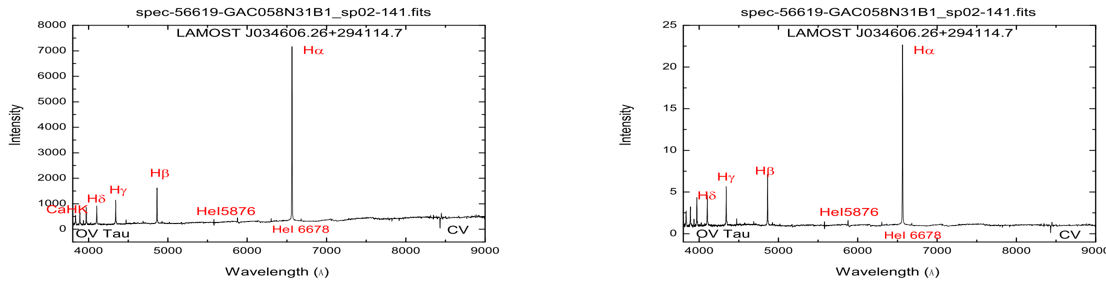

(f) CV: LAMOST J034606.26+294114.7

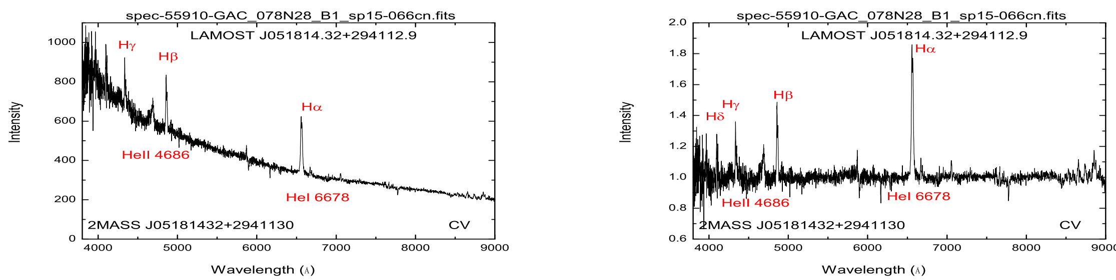

(g) CV: LAMOST J051814.32+294112.9

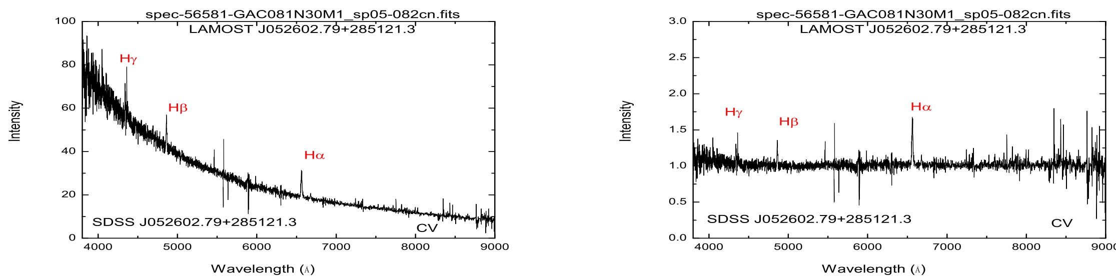

(h) CV: LAMOST J052602.79+285121.3

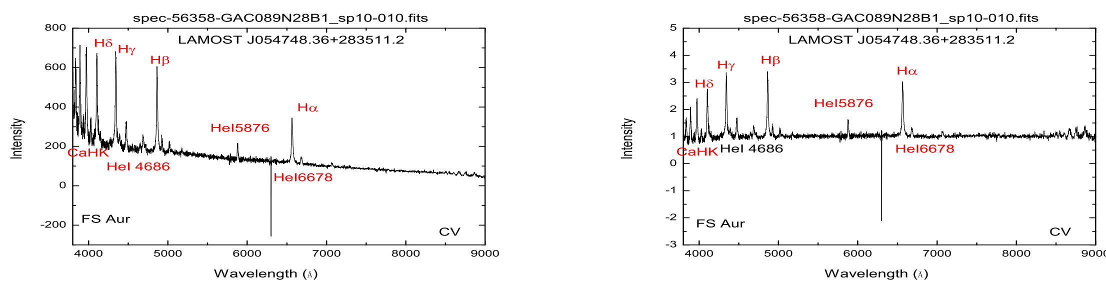

(i) CV: LAMOST J054748.36+283511.2

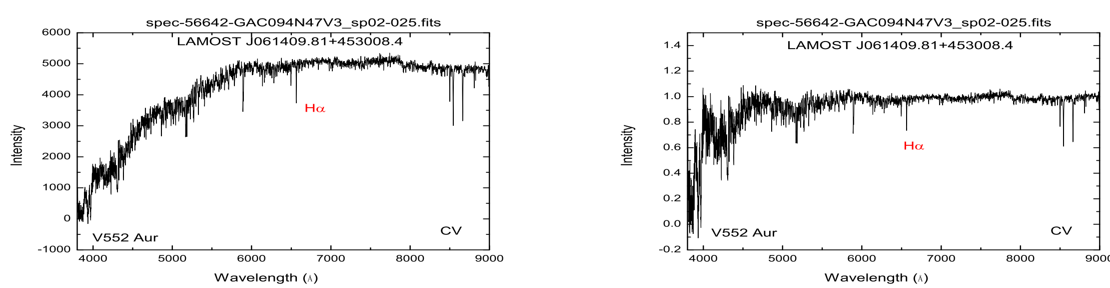

(j) CV: LAMOST J061409.81+453008.4

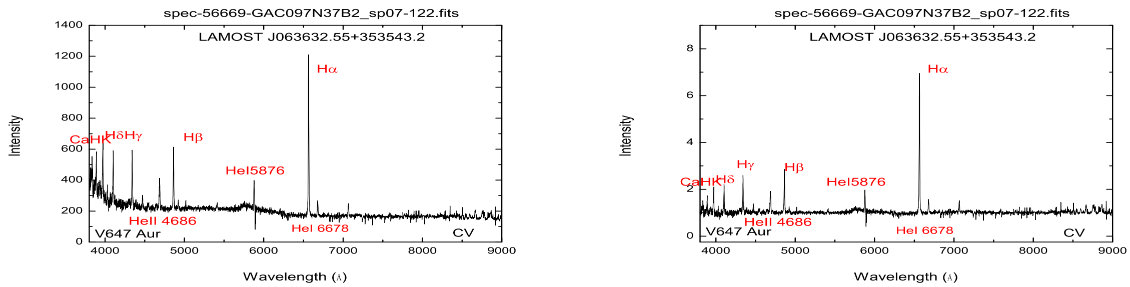

(k) CV: LAMOST J063632.55+353543.2

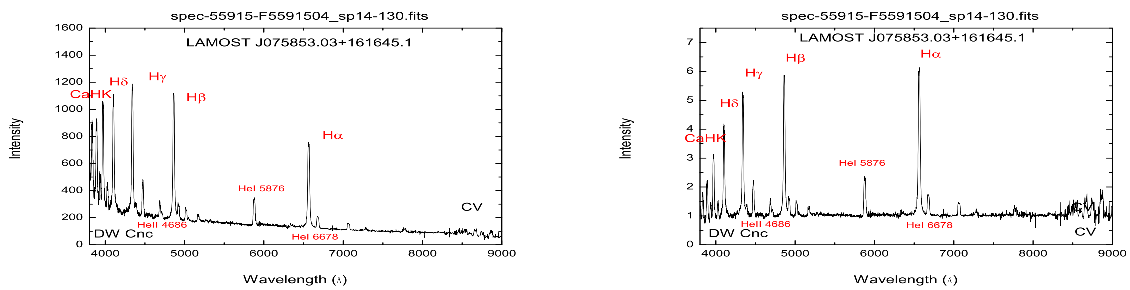

(l) CV: LAMOST J075853.03+161645.1

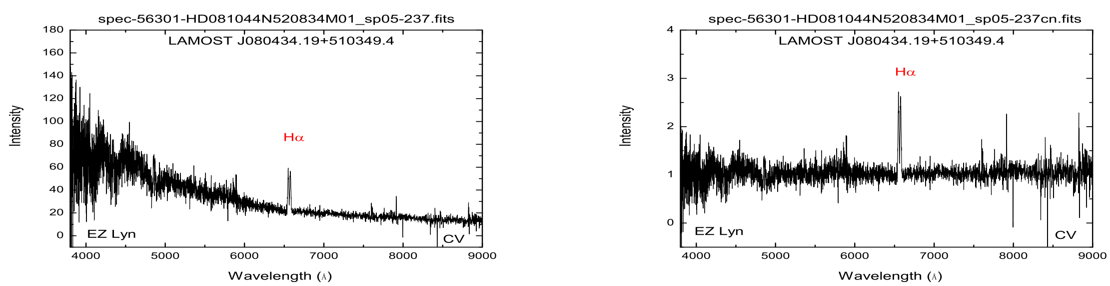

(m) CV: LAMOST J080434.19+510349.4

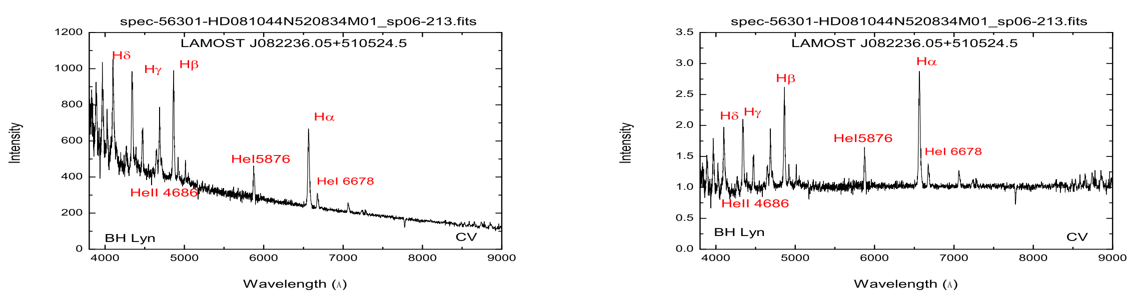

(n) CV:LAMOST J082236.05+510524.5

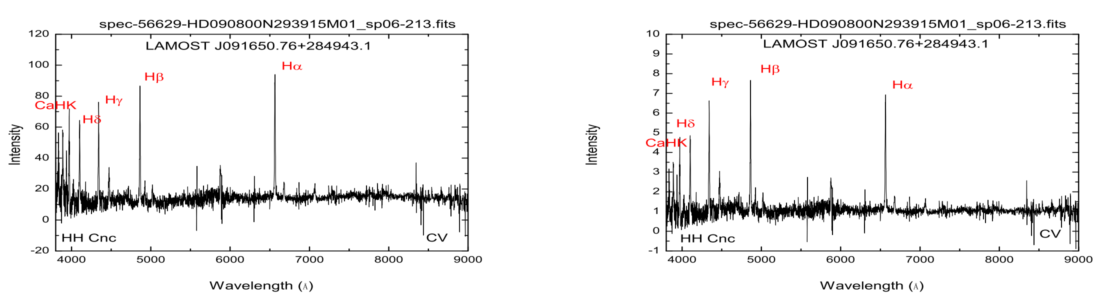

(o) CV: LAMOST J091650.76+284943.1

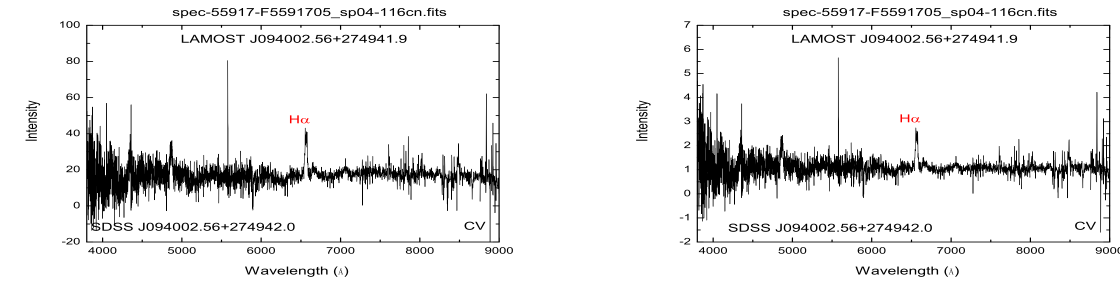

(p) CV: LAMOST J094002.56+274941.9

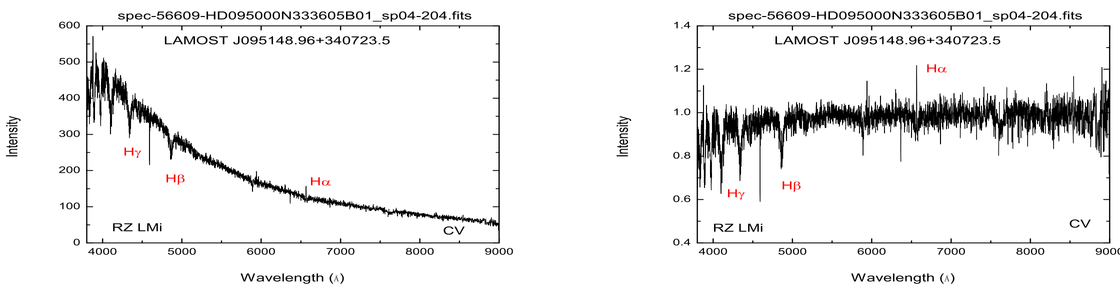

(q) CV: LAMOST J095148.96+340723.5

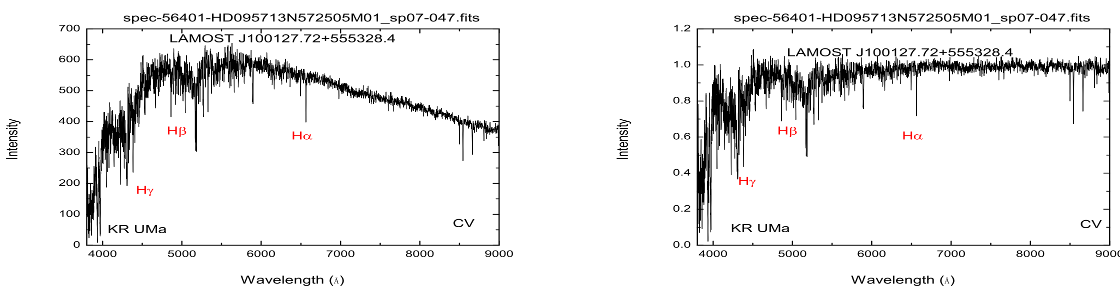

(r) CV: LAMOST J100127.72+555328.4

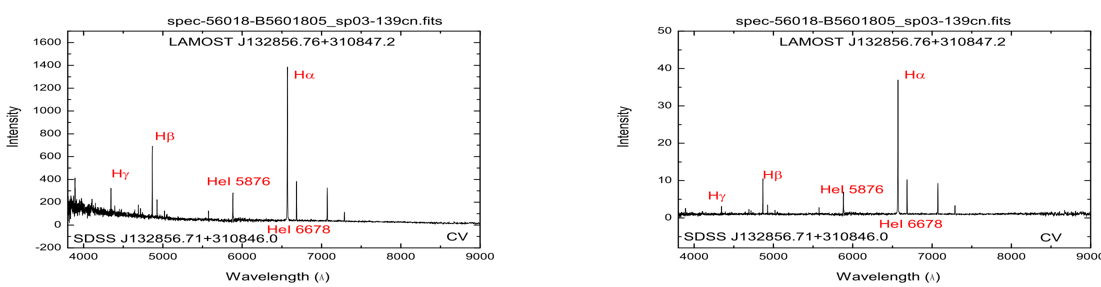

(s) CV: LAMOST J132856.76+310847.2

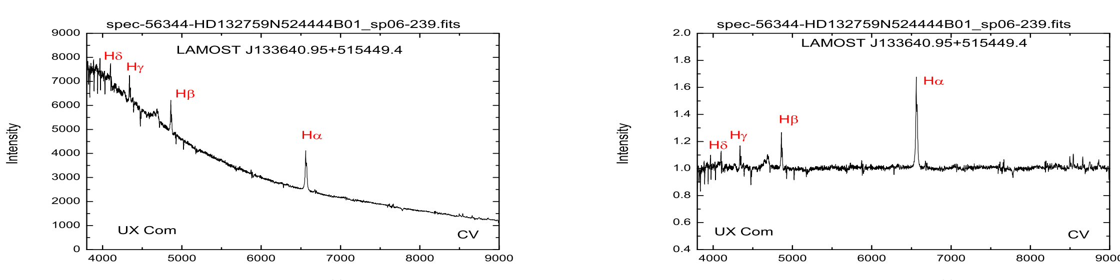

(t) CV: LAMOST J133640.95+515449.4

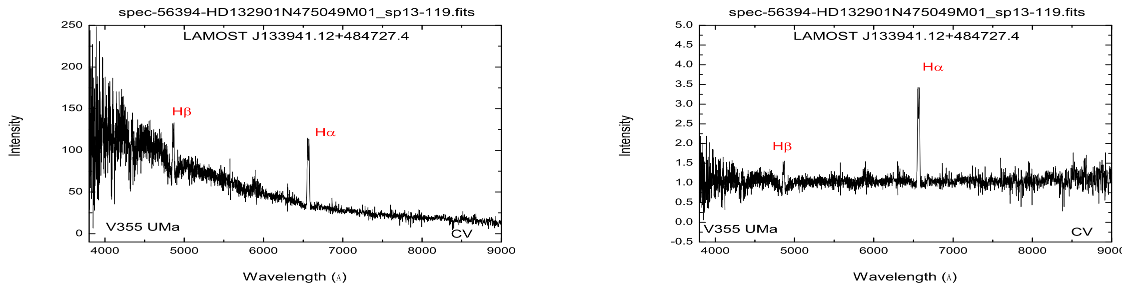

(u) CV: LAMOST J133941.12+484727.4

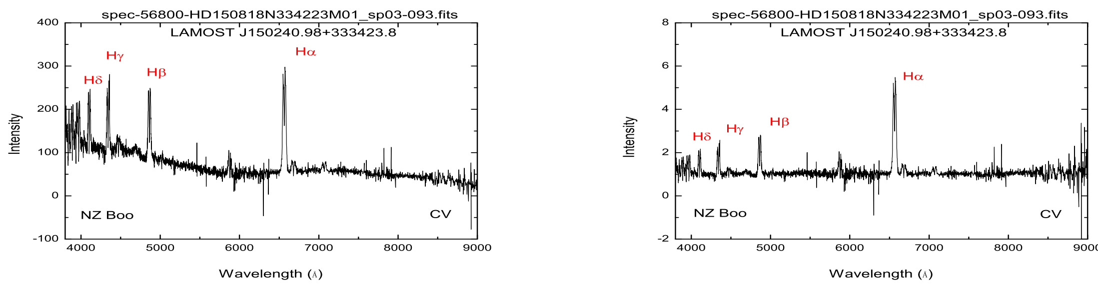

(v) CV: LAMOST J150240.98+333423.8

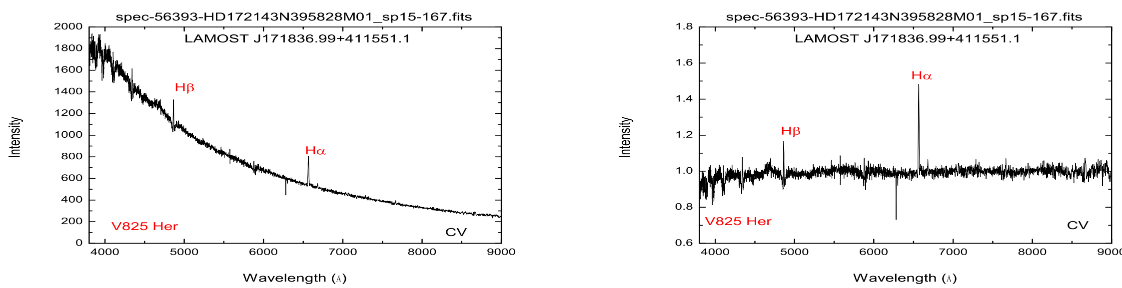

(w) CV: LAMOST J171836.99+411551.1

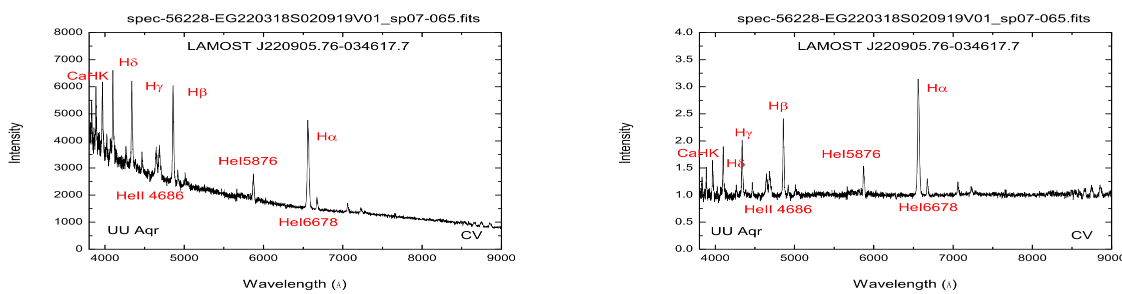

(x) CV: LAMOST J220905.76–034617.7

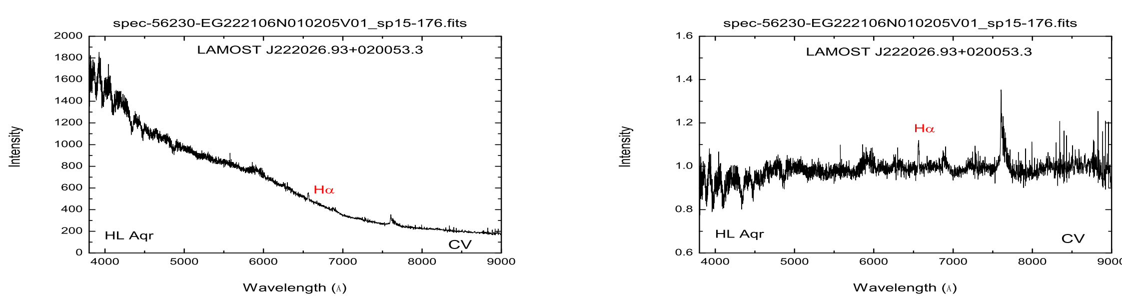

(y) CV: LAMOST J222026.93+020053.3

Fig. 1 CV samples with only one LAMOST spectrum. The observed spectra are shown in the *left panels*; the continuum-normalized ones are shown in the *right panels*. The LAMOST object names are written at the *top-center* inside the *rectangular plotting area*, and their commonly known names are written at the *lower-left corners* inside the *rectangular plotting area*.

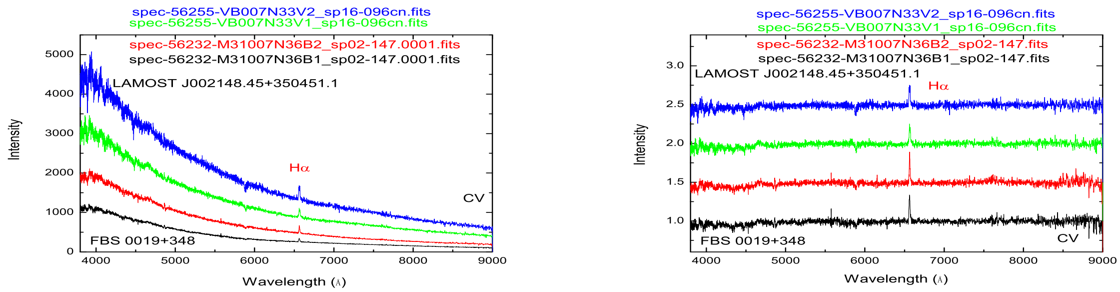

(a) LAMOST J002148.45+350451.1cv

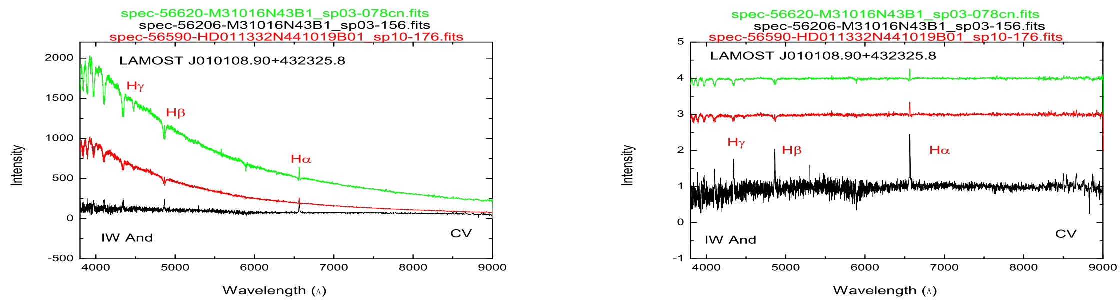

(b) LAMOST J010108.90+432325.8cv

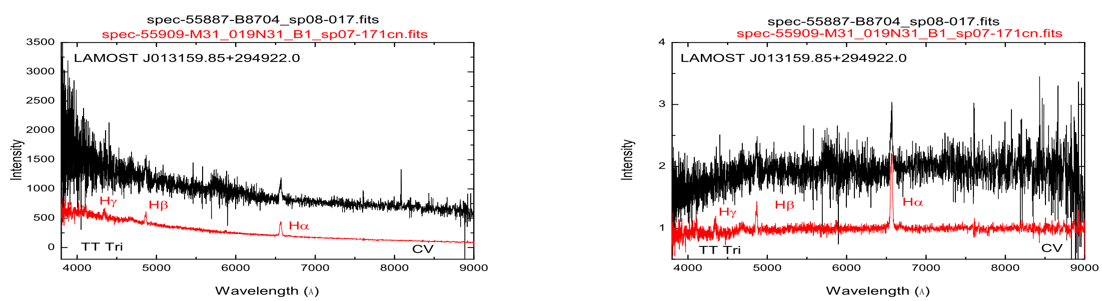

(c) LAMOST J013159.85+294922.0cv

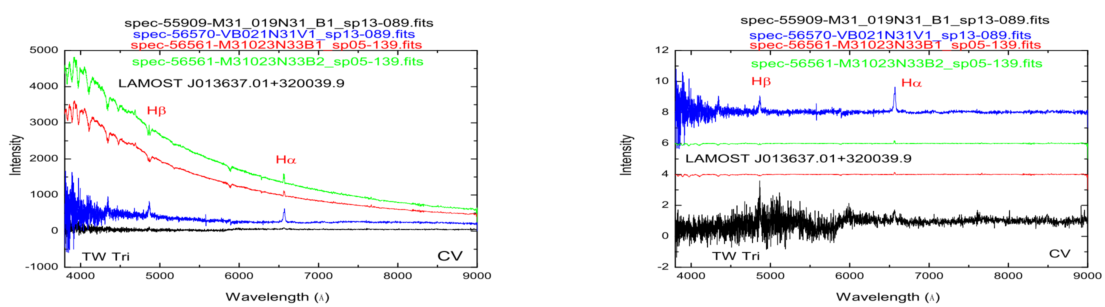

(d) LAMOST J013637.01+320039.9cv

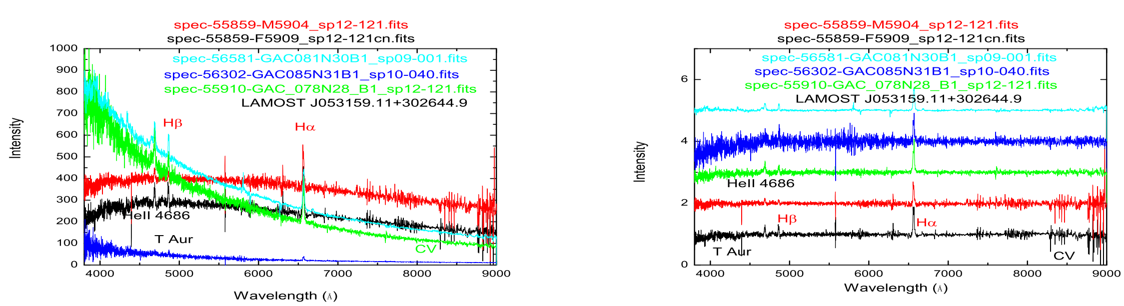

(e) LAMOST J053159.11+302644.9

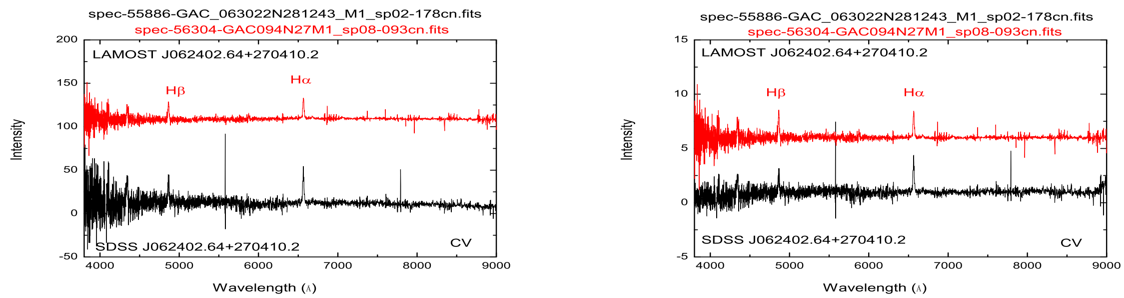

(f) LAMOST J062402.64+270410.2

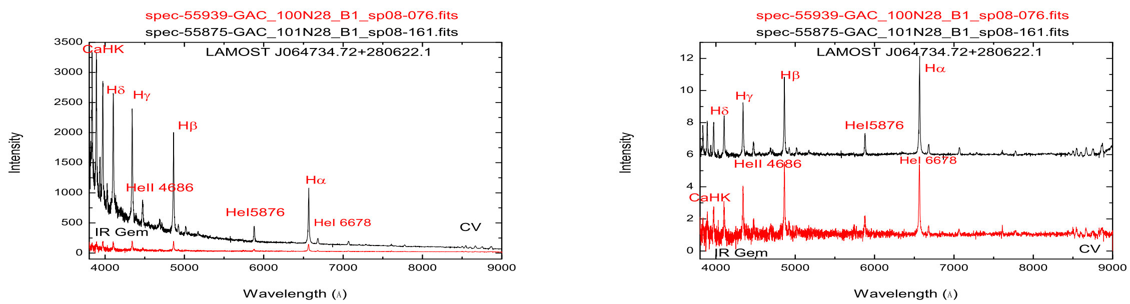

(g) LAMOST J064734.72+280622.1cv

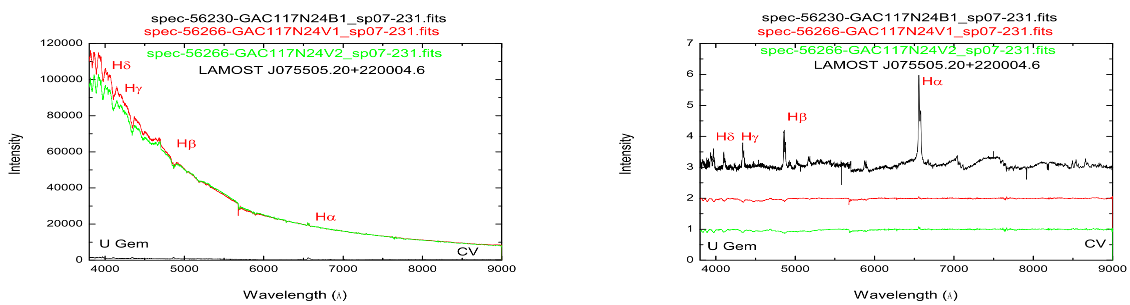

(h) LAMOST J075505.20+220004.6

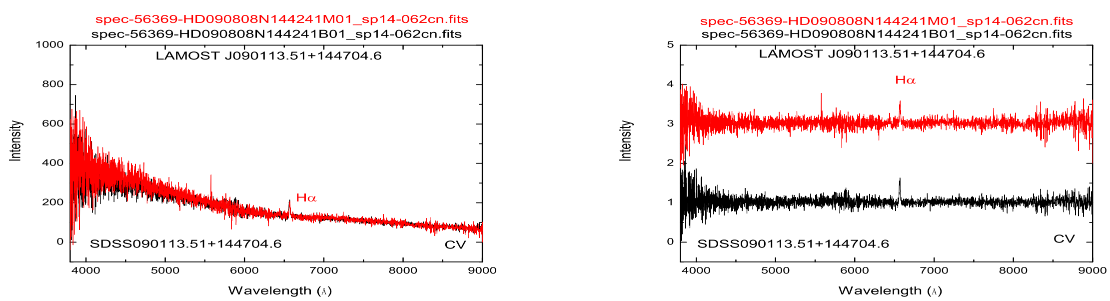

(i) LAMOST J090113.51+144704.6

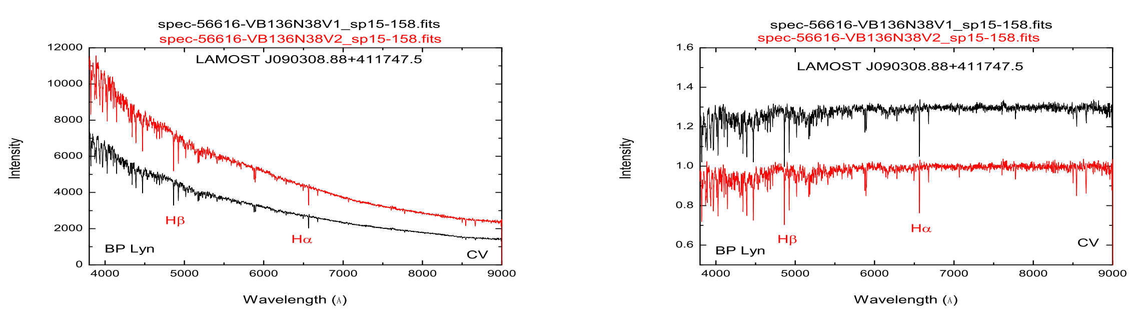

(j) LAMOST J090308.88+411747.5

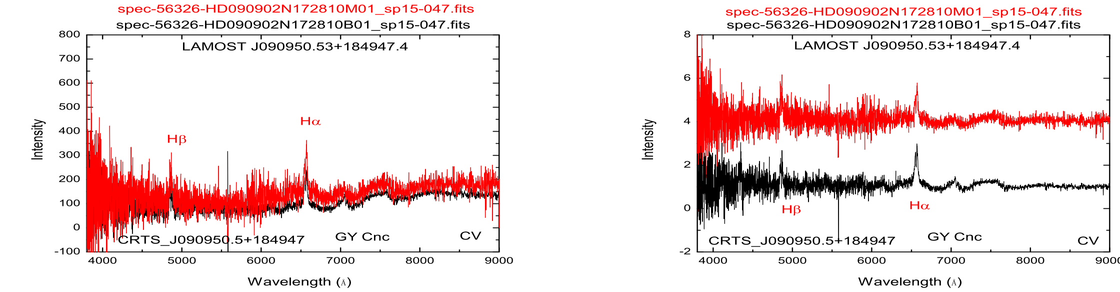

(k) LAMOST J090950.53+184947.4cv

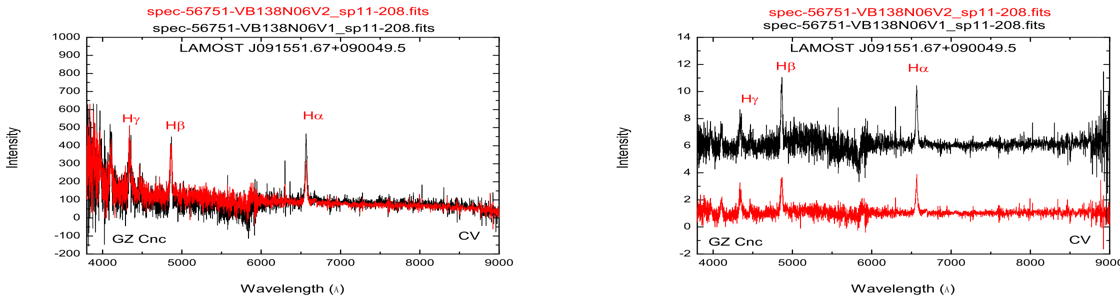

(l) LAMOST J091551.67+090049.5cv

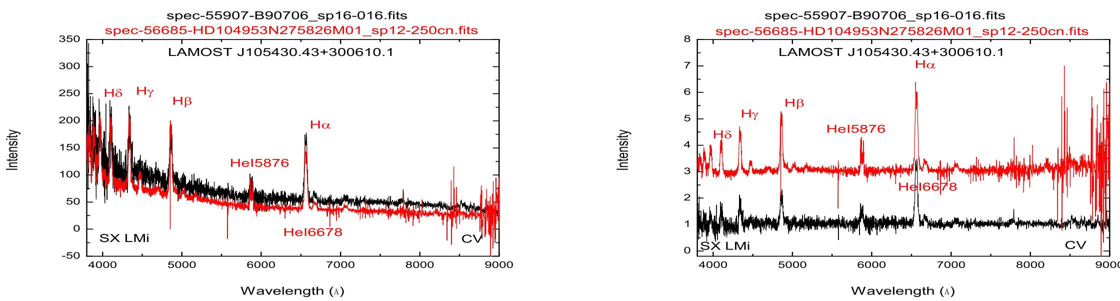

(m) LAMOST J105430.43+300610.1cv

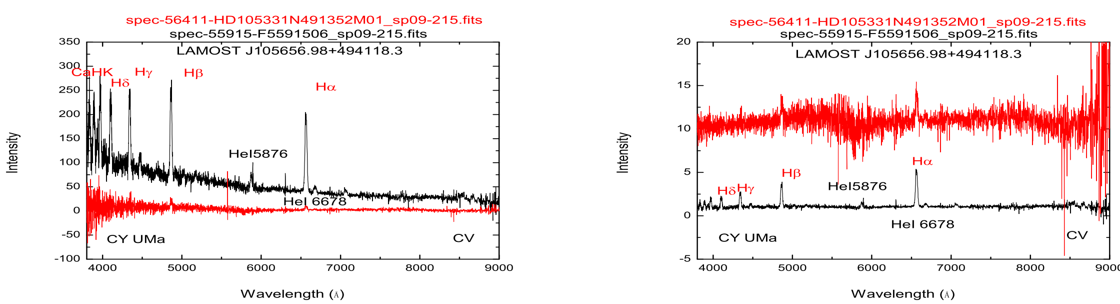

(n) LAMOST J105656.98+494118.3cv

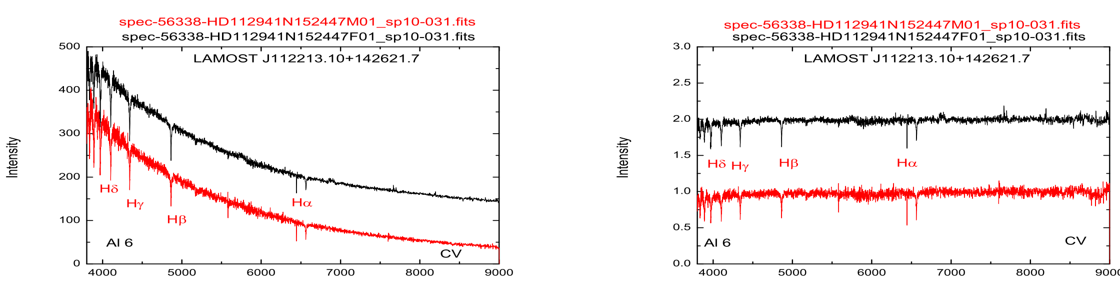

(o) LAMOST J112213.10+142621.7cv

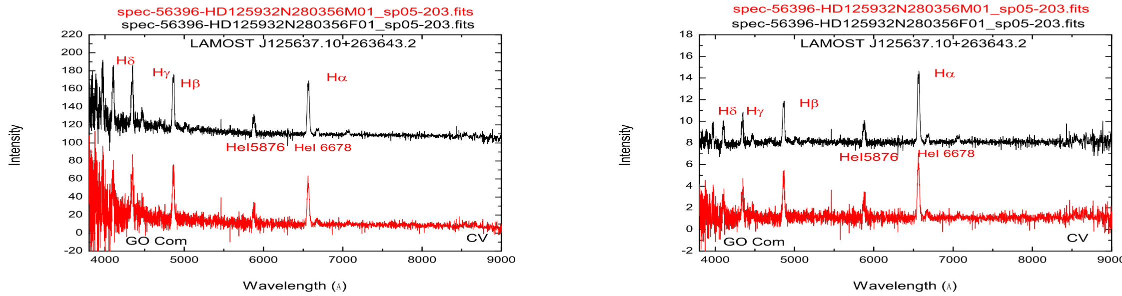

(p) LAMOST J125637.10+263643.2cv

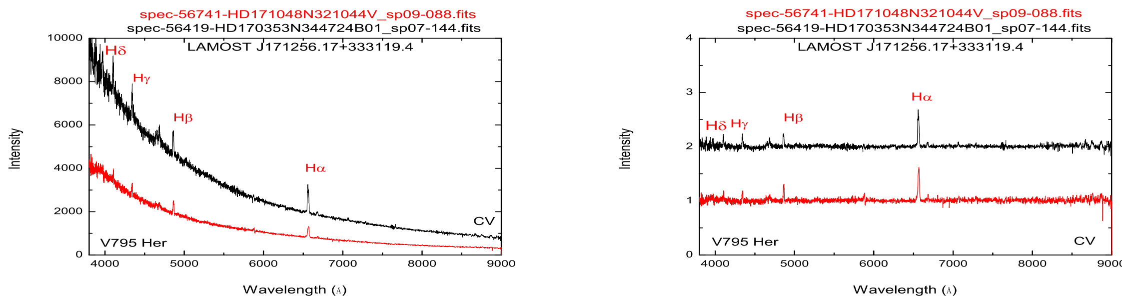

(q) LAMOST J171256.17+333119.4cv

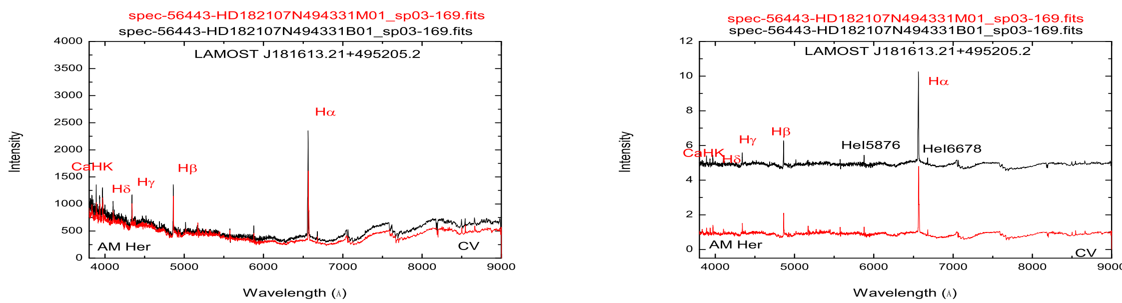

(r) LAMOST J181613.21+495205.2cv

Fig. 2 CV samples with two or more LAMOST spectra. The observed spectra are shown in the *left panels*; the continuum-normalized ones are shown in the *right panels*. Different colors represent spectra acquired at different observing times. Some of them show obvious emissions in several H Balmer and He I lines.

3.2 CVs Selected for Our Photometric Follow-up Observations

In order to study the periods and period variations of CVs, we carried out photometric follow-up observations for several CVs using the SARA RM 1.0 meter telescope (Keel et al. 2017), Xinglong 85-cm telescope, administered by National Astronomical Observatories, Chinese Academy of Sciences (NAOC) (Zhou et al. 2009) and Lijiang 2.4-m telescope, administered by Yunnan Observatories (Fan et al. 2015). SARA RM has a CCD camera with a 2048×2048 resolution and $11.6' \times 11.6'$ field of view, and limiting magnitude of 21 mag at S/N about 10 with a 10 min exposure time. The 85-cm Xinglong telescope has a CCD camera with 1024×1024 resolution, and $16.5' \times 16.5'$ field of view and limiting magnitude of about 15 mag with uncertainty about 0.005 mag in the R filter (before 2014). The Lijiang 2.4-m telescope has a PICCD camera with 1024×1024 pixels (Fan et al. 2015). Due to the limiting magnitudes of our telescopes and observing times, we selected five bright CVs as our photometric follow-up objects (UU Aqr, TT Tri, PX And, BP Lyn and RW Tri). Details about the observations for these five CVs are listed in Table 3. The backgrounds of these objects are described in the following subsections.

3.2.1 UU Aqr

UU Aqr was found to be a bright eclipsing nova-like CV (Baptista et al. 1994). It displayed short and long-term brightness variations (Honeycutt et al. 1998), with

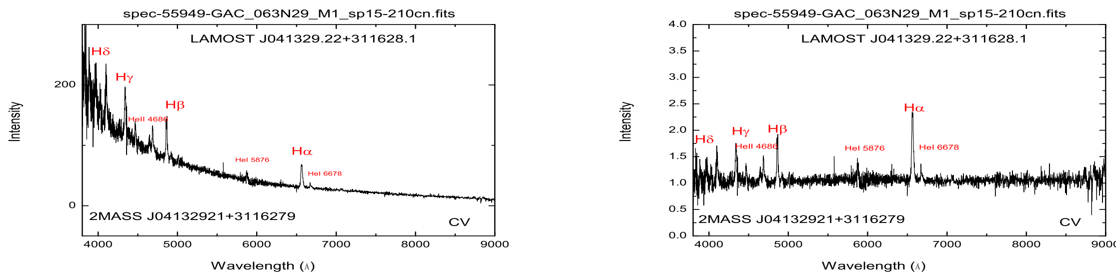

(a) NewCV: LAMOST J041329.22+311628.1

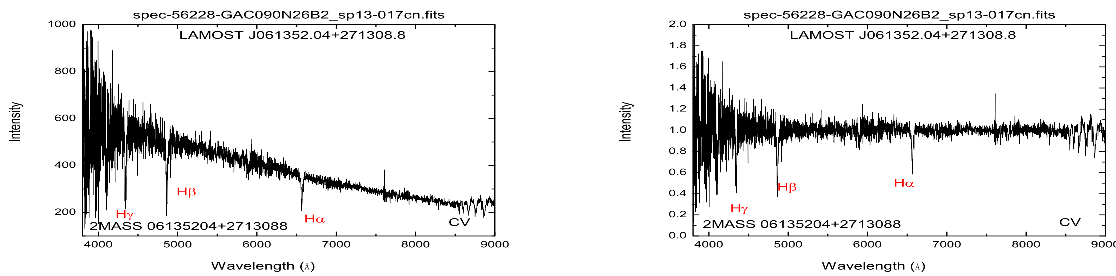

(b) NewCV: LAMOST J061352.04+271308.8

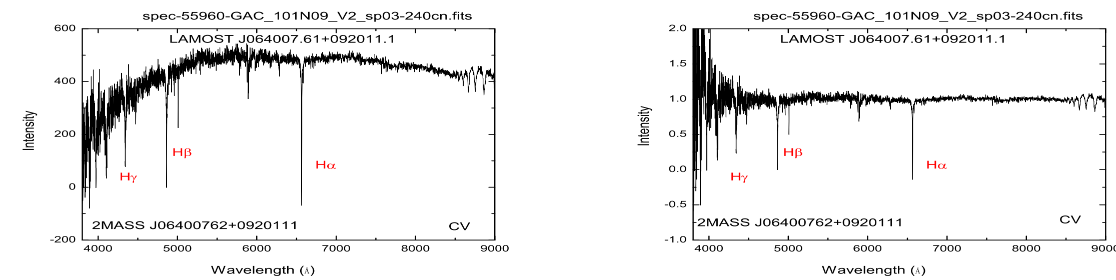

(c) NewCV: LAMOST J064007.61+092011.1

Fig. 3 New CV candidates observed by the LAMOST survey. The observed spectra are shown in the *left panels* and their the continuum-normalized ones are shown in the *right panels*.

occasional super humps in its light curve (Patterson et al. 2005). By analyzing 31 light curves of UU Aqr and using eclipsing mapping techniques, Baptista & Bortoletto (2008) found UU Aqr exhibited long-term brightness changes and flickering components. Dobrotka et al. (2012) also proposed a tantalizing explanation for the possible presence of spiral waves in the flickering activity of UU Aqr. These unstable light curves might be caused by spiral arms in the disk (Khruzina et al. 2015). Baptista et al. (2000) obtained time-resolved spectra of UU Aqr, which showed variable spectral lines from deep and narrow absorption features to emissions in Hα and He I lines (Baptista et al. 2000).

3.2.2 PX And

PX And was found to be a CV candidate (Green et al. 1982). It was confirmed to be a cataclysmic eclipsing binary with a period of 0.146 d (Li et al. 1990). There are strong variabilities in depths in the metal, Balmer and He lines (Thorstensen et al. 1991). Hellier & Robinson (1994) discovered that the emission line profile of Hα showed obvious absorption in different orbital phases. Still et al. (1995) presented time resolved spectroscopy of PX And in the 4025–5005 Å region and they argued that single peaked emission lines are incompatible with an accretion disk (absorption). Stanishev et al. (2002) conducted a photometric study, which indicated variable shape and depth in the eclipse, and strong flickering in the light curve outside eclipse.

3.2.3 TT Tri

TT Tri was identified as a new variable star in the constellation Triangulum (Romano 1978). Warren et al. (2006) provided multi-color light curves of the nova-like eclips-

Table 1 Parameters of CVs Observed in the LAMOST DR3 Spectroscopic Survey

No.	LAMOST name	Other name	First?	Date	Magnitudes								S/N					Ref.
				(d)	u	g	r	i	z	J	H	K	u	g	r	i	z	
(1)	(2)	(3)	(4)	(5)	(6)	(7)	(8)	(9)	(10)	(11)	(12)	(13)	(14)	(15)	(16)	(17)	(18)	(19)
cv01	LAMOST J002148.44+350451.1	FBS 0019+348	Y	2012-10-31	14.268	14.168	14.26	14.353	14.426	14.056	13.781	13.732	20.34	33.08	32.83	32.22	19.65	[1]
cv01	LAMOST J002148.45+350451.1	FBS 0019+348	Y	2012-10-31	14.268	14.168	14.26	14.353	14.426	14.056	13.781	13.732	22.04	30.56	24.11	15.41	11.64	[1]
cv01	LAMOST J002148.45+350451.2	FBS 0019+348	Y	2012-11-23	14.268	14.168	14.26	14.353	14.426	14.056	13.781	13.732	11.87	23.62	19.24	11.68	8.94	[1]
cv01	LAMOST J002148.45+350451.2	FBS 0019+348	Y	2012-11-23	14.268	14.168	14.26	14.353	14.426	14.056	13.781	13.732	14.15	28.91	25.08	17.78	14.35	[1]
cv02	LAMOST J003005.80+261726.3	PX And	N	2012-11-24	15.009	14.944	14.881	15.054	15.162	14.652	14.485	14.344	6.44	6.92	7.87	5.89	6.06	[2]
cv03	LAMOST J003135.88+434905.3	HQ And	N	2012-12-4						15.252	15.185	15.111	11.35	26.44	25.84	28.49	16.13	[1]
noncv01	LAMOST J004818.98+394111.7	IO And	N	2011-10-28	16.667	16.651	16.191	15.562	15.571	14.553	13.624	12.669	3.27	12.4	15.87	24.04	15.34	[1]
noncv01	LAMOST J004818.99+394111.7	IO And	N	2012-10-20	16.667	16.651	16.191	15.562	15.571	14.553	13.624	12.669	1.21	2.57	3.76	6.42	4.23	[1]
cv04	LAMOST J010108.90+432325.8	IW And	N	2012-10-5	14.886	14.565	14.709	14.819	14.896	15.005	14.676	14.529	2.18	4.48	7.51	10.65	8.78	[1]
cv04	LAMOST J010108.90+432325.8	IW And	N	2013-11-23	14.886	14.565	14.709	14.819	14.896	15.005	14.676	14.529	44.05	74.49	64.67	70.92	45.48	[1]
cv04	LAMOST J010108.93+432325.6	IW And	N	2013-10-24	14.886	14.565	14.709	14.819	14.896	15.005	14.676	14.529	23.59	41.3	37.86	38.4	24.41	[1]
noncv02	LAMOST J010959.21+280124.4	2MASS J01095921+2801244	Y	2012-12-5	16.731	15.592	15.214	15.085	15.04	14.225	13.923	13.83	2.44	20.22	39.18	47.6	28.94	[1]
cv05	LAMOST J013159.85+294922.0	TT Tri	N	2011-12-13	15.336	15.218	15.118	15.115	15.098	14.608	14.389	14.271	5.54	15.72	20.84	22.27	15.3	[1]
cv05	LAMOST J013159.85+294922.0	TT Tri	N	2011-11-21	15.336	15.218	15.118	15.115	15.098	14.608	14.389	14.271	1.52	3.76	4.17	4.97	2.66	[1]
cv06	LAMOST J013637.01+320040.0	TW Tri	N	2013-9-25	14.468	14.301	14.384	14.441	14.506	14.565	13.99	13.722	96.89	207.54	218	219.23	150.75	[1],[2]
cv06	LAMOST J013637.01+320039.9	TW Tri	N	2013-9-25	14.468	14.301	14.384	14.441	14.506	14.565	13.99	13.722	90.38	185.77	183.99	166.46	105.56	[1]
cv06	LAMOST J013637.01+320040.0	TW Tri	N	2011-12-13	14.468	14.301	14.384	14.441	14.506	14.565	13.99	13.722	1.5	1.69	3.81	4.33	4.03	[1]
cv06	LAMOST J013637.01+320039.9	TW Tri	N	2013-10-4	14.468	14.301	14.384	14.441	14.506	14.565	13.99	13.722	1.29	5.24	10.66	16.68	12.23	[1]
cv07	LAMOST J013737.21+300248.6	TX Tri	N	2011-12-22	17.772	17.49	16.771	16.447	16.271	15.035	14.611	14.479	3.95	13.35	19.21	31.26	24.95	[1],[4]
cv08	LAMOST J014304.65+263833.2	CRTS J014305+263833	N	2014/1/1	17.6	17.912	17.912	17.709	17.592				13.86	20.49	20.35	22.46	11.09	[3]
cv09	LAMOST J022536.15+280550.8	RW Tri	N	2013/10/6						11.938	11.578	11.46	5.37	14.83	26.34	39.65	28.96	[1]
noncv03	LAMOST J034300.28+573356.0	CW Cam	Y	2013-9-23						7.74	7.649	7.535	478.68	951.24	841.37	999	902.43	[1]
cv11	LAMOST J034313.84+240509.3	V1209 Tau	Y	2012-10-12						14.941	14.584	14.321	1.6	7.17	13.24	17.96	11.94	[1]
cv12	LAMOST J034606.26+294114.7	OV Tau	N	2013-11-22						11.951	11.013	10.346	9.41	21.75	57.71	99.91	96.05	[1]
newcv01	LAMOST J041329.22+311628.1	2MASS J04132921+3116279	Y	2012/1/22						16.286	16.128	15.7	3.72	14.33	8.64	8.72	4.96	[3]
noncv04	LAMOST J042112.14+162616.7	CRTS J042112.1+162616	Y	2014-1-23	19.485	16.668	14.544	11.869	10.336	7.755	6.795	6.208	5.38	25.05	127.47	512.43	709.93	[1]
noncv05	LAMOST J044954.16+403230.6	NSV 1725	N	2013-2-19						12.361	12.277	12.208	4.68	24.27	30.23	31.17	32.72	[1]
cv13	LAMOST J051814.32+294112.9	2MASS J05181432+2941130	N	2011/12/14						13.872	13.518	13.274	5.71	19.37	30.39	37.12	29.96	[3]
cv14	LAMOST J052602.79+285121.3	SDSS J052602.79+285121.3	Y	2013/10/15	18.732	18.271	17.735	17.653	17.588	16.502	16.414	15.947	3.95	14.1	17.19	19.72	10.4	[4]
...	...	...	...	...	...	...	...	...	...	...	...	...	...	...	...	...	...	...

Notes: This is a partial list of CVs. The parameters and the full list are available at *http://www.raa-journal.org/docs/Supp/RAA4138Table1*. Reference: CV Catalog 1. Downes et al. 2001; 2. CRTS (Breedt et al. 2014); 3. LAMOST new cv candidates (Luo et al. 2015); 4. SDSS (Szkody et al. 2011). Here, cv means known cv. Noncv means a non-cv object in the cv catalog published by Downes et al. (2001). Y in the fourth column means that this is the first time this spectrum has been observed by LAMOST, while N means this not the first time this spectrum has been observed.

ing binary TT Tri and obtained their associated geometry models. Rodríguez-Gil et al. (2007) presented a revised and more accurate orbital period and found that Balmer and He I lines showed emissions.

3.2.4 BP Lyn

BP Lyn was found to be a nova-like variable with an orbital period of about 3.7 h (Grauer et al. 1994) and its light curve showed prominent flickering. Wegner &

Table 2 EWs of Several Spectral Emission Lines for CVs Observed in the LAMOST Survey

No	LAMOST name	HJD (24,) (d)	EW (Hα) (Å)	Variation	EW (Hβ) (Å)	EW (Hγ) (Å)	EW (Hδ) (Å)	EW (HeI 5876) (Å)	EW (HeI 6678) (Å)	EW (Hα) (Å)	EW (Hβ) (Å)	Ref.
(1)	(2)	(3)	(4)	(5)	(6)	(7)	(8)	(9)	(10)	(11)	(12)	(13)
cv01	LAMOST J002148.44+350451.1	56231	+5.431 ± 0.021	01v	–	–	–	–	–			
cv01	LAMOST J002148.45+350451.1	56231	+4.902 ± 0.127	01v	–	–	–	–	–			
cv01	LAMOST J002148.45+350451.2	56254	+4.300 ± 0.217	01v	–	–	–	–	–			
cv01	LAMOST J002148.45+350451.2	56254	+4.191 ± 0.108	01v	–	–	–	–	–			
cv02	LAMOST J003005.80+261726.3	56255	+52.244 ± 0.824	02v	+25.081 ± 0.709	+17.091± 0.309	+11.950± 0.440	–	–		16.7–24.3	[1]
cv03	LAMOST J003135.88+434905.3	56265	+4.670 ± 0.153	03v	–	–	–	–	–	8.8	1.5	[2]
noncv01	LAMOST J004818.98+394111.7	55862	–	–	–	–	–	–	–			
noncv01	LAMOST J004818.99+394111.7	56220	–	–	–	–	–	–	–			
cv04	LAMOST J010108.90+432325.8	56205	+20.782 ± 1.502	04v	+8.991 ± 0.065	+5.533± 0.746	–	–	–	absorption	core emission	[2]
cv04	LAMOST J010108.90+432325.8	56619	+1.683 ± 0.044	04v	core ±	–	+7.279± 0.026	–	–			
cv04	LAMOST J010108.93+432325.6	56589	+2.573 ± 0.079	04v	core ±	–	–	–	–			
noncv02	LAMOST J010959.21+280124.4	56266	–3.739 ± 0.801	–	– 4.937±1.005	–	–	–	–			
cv05	LAMOST J013159.85+294922.0	55908	+34.839 ± 0.289	05v	+7.819 ± 0.296	+6.271± 0.754	–	–	–	22.536		[3]
cv05	LAMOST J013159.85+294922.0	55886	+24.053 ± 1.027	05v	–	–	–	–	–			
cv06	LAMOST J013637.01+320040.0	56560	+1.980 ± 0.120	06v	–3.850 ± 0.67	–4.391± 0.286	–6.345± 0.032	–	–	38	38	[4]
cv06	LAMOST J013637.01+320039.9	56560	+2.141 ± 0.133	06v	core ±	–4.138± 0.170	–50.775± 4.706	– 0.791 ± 0.18	–			
cv06	LAMOST J013637.01+320040.0	55908	+15.871 ± 0.239	06v	–	–	–	–	–			
cv06	LAMOST J013637.01+320039.9	56569	+37.548 ± 1.708	06v	+13.415 ± 0.635	–	–	–	–			
cv07	LAMOST J013737.21+300248.6	55917	+47.730 ± 9.620	07v	+45.413 ± 8.333	+40.384± 7.214	+32.691± 4.181	+9.603± 0.65	–	8.5	emission	[5]
cv08	LAMOST J014304.65+263833.2	56658	+90.779 ± 9.539	08v	+76.436 ± 7.756	+71.659± 10.919	+36.851 ± 1.231	+20.986± 1.666	–	75	emission	[6]
cv09	LAMOST J022536.15+280550.8	56571	+59.754 ± 3.984	–	+24.891 ± 0.191	+13.648± 0.182	+8.767 ± 0.103	+5.155± 0.365	–	emission	emission	[7]
noncv03	LAMOST J034300.28+573356.0	56558	–	–	–	–	–	–	–			
cv11	LAMOST J034313.84+240509.3	56212	–2.778 ± 0.030	–	–	–	–	–	–			
cv12	LAMOST J034606.26+294114.7	56618	+125.628 ± 9.928	–	+39.815 ± 8.225	+30.877± 6.047	+23.627± 2.967	–	–	emission	emission	[8]
newcv01	LAMOST J041329.22+311628.1	55948	+41.038 ± 1.988		+17.839 ± 0.249	+15.087± 0.993	+12.054 ± 0.086	+6.666± 3.166	–			
noncv04	LAMOST J042112.14+162616.7	56680	–	–	–	+18.078± 4.228	+31.295± 0.565	–	–			
noncv05	LAMOST J044954.16+403230.6	56342	–11.959 ± 0.499	–	–18.588 ± 0.558	–17.634±0.394	–21.620± 0.99	–	–			
cv13	LAMOST J051814.32+294112.9	55909	+24.798 ± 1.188	–	+8.312 ± 0.577	+4.697± 0.717	+1.803 ± 0.221	+1.289± 0.159	–	emission	emission	[9]
cv14	LAMOST J052602.79+285121.3	56580	+12.327 ± 0.957	–	+3.719 ± 0.034	+2.367± 0.254	–	–	–			[7]
cv15	LAMOST J053159.11+302644.9	55858	+11.326 ± 0.034	09v	–	–	–	–	–		2.9–7.7	[10]
...	...	...	...	...	...	...	...	...	...	...	...	

Notes: V means that there are variations in EWs; N means that there are no variations in EWs; – means that we do not discuss whether there is variation because of no repeated LAMOST spectra. [1] Still et al. (1995); [2] Liu et al. (1999); [3] Zhang et al. (2018); [4] Thorstensen et al. (1998); [5] Liu & Hu (2000); [6] Thorstensen et al. (2016); [7] Matthews et al. (2015); [8] Zwitter & Munari (1994); [9] Witham et al. (2007); [10] Bianchini (1980); [11] Austin et al. (2011); [12] Liu & Hu (2000); [13] Girven et al. (2011); [14] Gänsicke et al. (2005); [15] Lazaro et al. (1991); [16] Patterson et al. (2011); [17] Unda-Sanzana et al. (2006); [18] Szkody et al. (2006); [19] Patterson et al. (2004); [20] Isogai et al. (2015); [21] Dhillon et al. (1992); [22] Szkody et al. (2009); [23] Hoard & Szkody (1996); [24] Thorstensen (2000); [25] Szkody et al. (2009); [26] Sheets et al. (2007); [27] Szkody et al. (2007) [28] Szkody & Howell (1992); [29] Szkody et al. (2005); [30] Liu & Hu (2000); [31] Szkody et al. (2011); [32] Kjurkchieva et al. (2006); [33] Szkody (2015); [34] Casares et al. (1996); [35] Ringwald et al. (2005); [36] Skidmore et al. (2004); [37] Baptista et al. (2000); [38] Downes et al. (1995). This is a partial list. The complete parameter list is available at *http://www.raa-journal.org/docs/Supp/RAA4138Table2*.

Table 3 Observation Log of CVs

Target	Name	Exposure time (s)	RA(2000) and Dec(2000)	J	H	K	Reference
Variable	UU Aqr	15	22 09 05.76; –03 46 17.7	12.971	12.629	12.483	Skrutskie et al. (2006)
Comparison	2MASS J22091087-0347058	15	22 09 10.81; –03 47 06.5	10.731	10.423	10.319	Skrutskie et al. (2006)
Check	2MASS J22091311-0344361	15	22 09 13.07; –03 44 36.4	11.617	11.258	11.167	Skrutskie et al. (2006)
Variable	PX And	120	00 30 05.81; +26 17 26.4	14.652	14.485	14.344	Skrutskie et al. (2006)
Comparison	2MASS J00295436+2621175	120	00 29 54.36; +26 21 17.6	11.707	11.358	11.294	Skrutskie et al. (2006)
Check	2MASS J00300561+2620221	120	00 30 05.61; +26 20 22.0	12.433	12.130	12.047	Skrutskie et al. (2006)
Variable	TT Tri	60	01 31 59.86; +29 49 22.1	14.608	14.389	14.271	Skrutskie et al. (2006)
Comparison	2MASS J01315548+2950258	60	01 31 55.48; +29 50 26.3	11.483	10.897	10.796	Skrutskie et al. (2006)
Check	2MASS J01320204+2954117	60	01 32 02.05; +29 54 12.5	11.862	11.496	11.486	Skrutskie et al. (2006)
Variable	BP Lyn	50	09 03 08.89; +41 17 47.7	13.854	13.746	13.527	Skrutskie et al. (2006)
Comparison	2MASS J09025877+4124150	50	09 02 58.78; +41 24 15.2	12.865	12.665	12.620	Skrutskie et al. (2006)
Check	2MASS J09024774+4114349	50	09 02 47.76; +41 14 35.4	10.716	10.255	10.126	Skrutskie et al. (2006)
Variable	RW Tri	15–40	02 25 36.15; +28 05 50.9	12.140	11.770	11.590	Skrutskie et al. (2006)
Comparison	2MASS J02253174+2804065	15–40	02 25 31.71; +28 04 06.6	12.381	12.064	11.970	Skrutskie et al. (2006)
Check	2MASS J02253362+2806296	15–40	02 25 33.62; +28 06 30.0	12.853	12.478	12.449	Skrutskie et al. (2006)

Note: This table uses the Simbad and VizieR databases, operated at CDS, Strasbourg, France.

Table 4 CCD Observational Data on Five CVs

Star name	HJD$_U$	Δ Mag$_U$	HJD$_B$	Δ Mag$_B$	HJD$_V$	Δ Mag$_V$	HJD$_R$	Δ Mag$_R$	HJD$_I$	Δ Mag$_I$	Telescope
UU Aqr	2457614.44238	0.219	2457614.41829	0.792	2457614.41889	1.361	2457614.41921	1.475	2457614.41941	1.610	SARA RM 1m
UU Aqr	2457614.44528	0.256	2457614.41993	0.742	2457614.42053	1.250	2457614.42086	1.354	2457614.42105	1.504	SARA RM 1m
UU Aqr	2457614.44818	0.110	2457614.42157	0.647	2457614.42218	1.168	2457614.42250	1.381	2457614.42270	1.539	SARA RM 1m
UU Aqr	2457614.45110	0.145	2457614.42322	0.793	2457614.42382	1.321	2457614.42414	1.428	2457614.42434	1.556	SARA RM 1m
UU Aqr	2457614.45400	0.130	2457614.42486	0.633	2457614.42546	1.205	2457614.42579	1.311	2457614.42598	1.534	SARA RM 1m
UU Aqr	2457614.45691	0.108	2457614.43438	0.931	2457614.43499	1.441	2457614.43533	1.483	2457614.43565	1.625	SARA RM 1m
UU Aqr	2457614.45980	0.156	2457614.43625	0.831	2457614.43686	1.419	2457614.43720	1.597	2457614.43753	1.727	SARA RM 1m
UU Aqr	2457614.46271	0.022	2457614.43814	0.859	2457614.43874	1.408	2457614.43909	1.554	2457614.43940	1.764	SARA RM 1m
UU Aqr	2457614.46561	–0.045	2457614.44001	0.928	2457614.44073	1.423	2457614.44108	1.549	2457614.44142	1.758	SARA RM 1m
...	...	...	...	...	...	...	...	...	...	...	
PX And	2457636.52140	0.870	...	...	...	...	2457636.52140	0.765	...	...	SARA RM 1m
PX And	2457636.52216	0.910	...	...	...	...	2457636.52216	0.803	...	...	SARA RM 1m
PX And	2457636.52293	0.955	...	...	...	...	2457636.52293	0.841	...	...	SARA RM 1m
PX And	2457636.52369	0.956	...	...	...	...	2457636.52369	0.845	...	...	SARA RM 1m
...	...	...	...	...	...	...	...	...	...	...	
TT Tri	...	...	...	...	...	...	2457633.58859	1.899	...	...	SARA RM 1m
TT Tri	...	...	...	...	...	...	2457633.58936	1.877	...	...	SARA RM 1m
TT Tri	...	...	...	...	...	...	2457633.59013	1.881	...	...	SARA RM 1m
TT Tri	...	...	...	...	...	...	2457633.59090	1.899	...	...	SARA RM 1m
TT Tri	...	...	...	...	...	...	2457633.59166	1.926	...	...	SARA RM 1m
TT Tri	...	...	...	...	...	...	2457633.59243	1.957	...	...	SARA RM 1m
...	...	...	...	...	...	...	...	...	...	...	
BP Lyn	...	...	...	...	...	...	...	...	2455188.31472	1.145	Xinglong 85-cm
BP Lyn	...	...	...	...	...	...	...	...	2455188.31543	1.151	Xinglong 85-cm
BP Lyn	...	...	...	...	...	...	...	...	2455188.31614	1.162	Xinglong 85-cm
BP Lyn	...	...	...	...	...	...	...	...	2455188.31684	1.169	Xinglong 85-cm
BP Lyn	...	...	...	...	...	...	...	...	2455188.31755	1.172	Xinglong 85-cm
BP Lyn	...	...	...	...	...	...	...	...	2455188.31827	1.178	Xinglong 85-cm
RW Tri	...	...	...	...	...	...	2454820.98941	–0.078			Lijiang 2.4 m
RW Tri	...	...	...	...	...	...	2454820.98969	–0.087			Lijiang 2.4 m
RW Tri	...	...	...	...	...	...	2454820.98997	–0.088			Lijiang 2.4 m
RW Tri	...	...	...	...	...	...	2454820.99025	–0.095			Lijiang 2.4 m
RW Tri	...	...	...	...	...	...	2454820.99053	–0.08			Lijiang 2.4 m
RW Tri	...	...	...	...	...	...	2454820.99081	–0.058			Lijiang 2.4 m
...	...	...	...	...	...	...					

Notes: The full list of data points is available at *http://www.raa-journal.org/docs/Supp/RAA4138Table4*.

McMahan (1985) obtained its low resolution spectrum that showed emission in the Hα line. The Hα line profile showed complex emission features with a variable absorption component in the core (Still 1996; Hoard & Szkody 1996).

3.2.5 RW Tri

RW Tri was found to have a short period Algol type light curve variation outside eclipse (Walker 1963). Africano et al. (1978) recorded 30 eclipse minima for this star. By studying the associated $O - C$ diagram, they found that

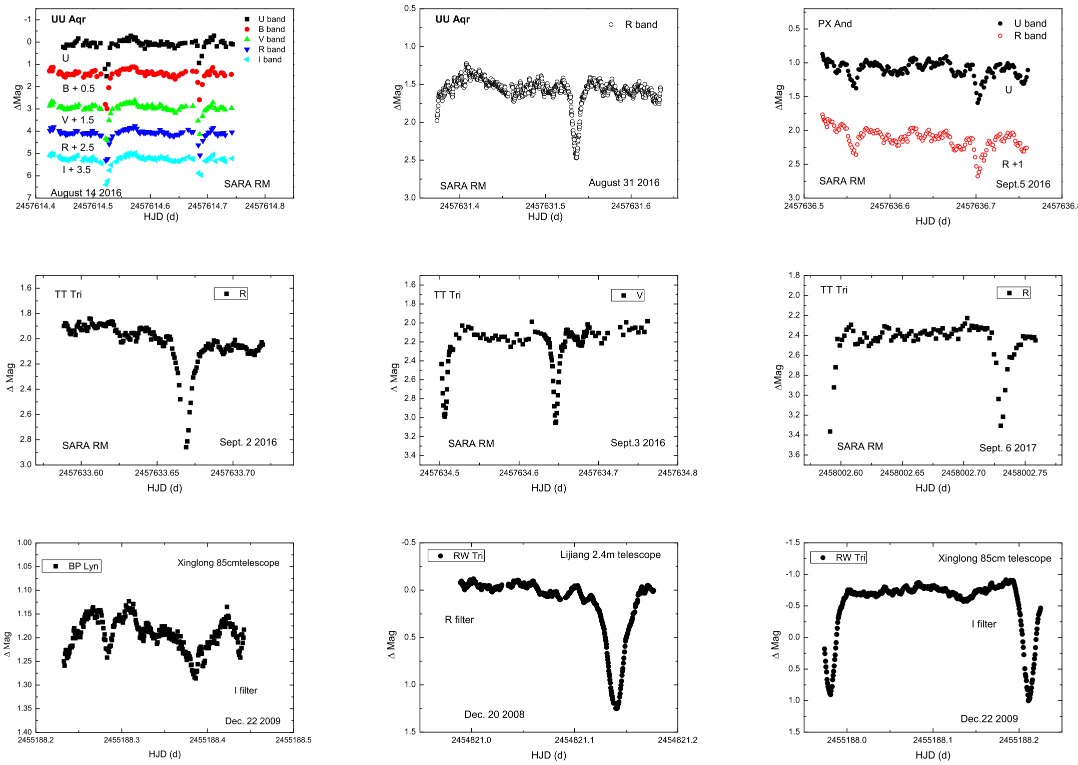

Fig. 4 Photometric follow-up light curves of UU Aqr, TT Tri, PX And, BP Lyn and RW Tri.

the minima contain oscillations with a peak amplitude of 0.0017 days with two possible periods of about 2777 days and 4980 days (Africano et al. 1978). RW Tri was found to have emissions in He II 4686, and Hα, Hβ and Hγ lines (Kaitchuck et al. 1983; Rutten & Dhillon 1992; Dhillon et al. 1992). Smak (1995) obtained the component masses of about 0.45(0.15) and 0.63(0.10) $M_{\odot}$. Rutten et al. (1992) derived the masses of RW Tri components of about 0.7 and 0.6 $M_{\odot}$ with an inclination of 75°. Recently, Poole et al. (2003) estimated the primary and secondary star masses to be in the range 0.4–0.7 and 0.3–0.4 $M_{\odot}$, respectively.

As can be seen from Figures 1 and 2, there were strong emissions from PX And in the Hα, Hβ, Hγ, Hδ and He I 4471, 4686, 6678 and 5876 Å lines (Fig. 1a). UU Aqr showed strong emissions in the Hα, Hβ, Hγ, Hδ and He I 4471, 4686, 6678 and 5876 Å and Ca II IRT lines (Fig. 1x), while TT Tri presented strong emissions in the Hα, Hβ and Hγ lines (Fig. 2c). Hence, we confirm their previously reported behaviors in the Balmer and He I lines (Still et al. (1995), Baptista et al. (2000), Rodríguez-Gil et al. (2007), etc). However, this is the first time ever that emissions in the Ca II IRT lines for UU Aqr have been reported. For BP Lyn, there are obvious absorptions in the Hα and Hβ lines. There are strong emissions from RW Tri in the Hα, Hβ, Hγ, Hδ and He I 6678 and 5876 Å lines (Fig. 1e). We confirm their previously reported behaviors in the Balmer lines (Dhillon et al. 1992; etc).

3.3 Photometric Follow-up Observations of CVs

We carried out CCD observations of UU Aqr in $UBVRI$ on 2016 August 13 using the SARA RM 1.0 meter telescope (Keel et al. 2017). However, the time resolution is not very good due to its short orbital period. Therefore, we observed it again only utilizing the R filter on 2016 August 16. We made the CCD observation for PX And in two colors with UR filters on 2016 September 5 using the SARA RM 1.0 meter telescope. We observed TT Tri in only one color on 2016 September 2 and 3, and 2017 September 6 employing the SARA RM 1.0 meter telescope. We also conducted photometric studies of BP Lyn in I filter using the Xinglong 85-cm telescope (Zhou et al. 2009). In addition, we performed studies of RW Tri in R filter using the 2.4-m telescope on 2008 December 20 and in I filter using the Xinglong 85-cm telescope on 2009 December 22. The observation log of our objects, including the exposure times, is listed in Table 3.

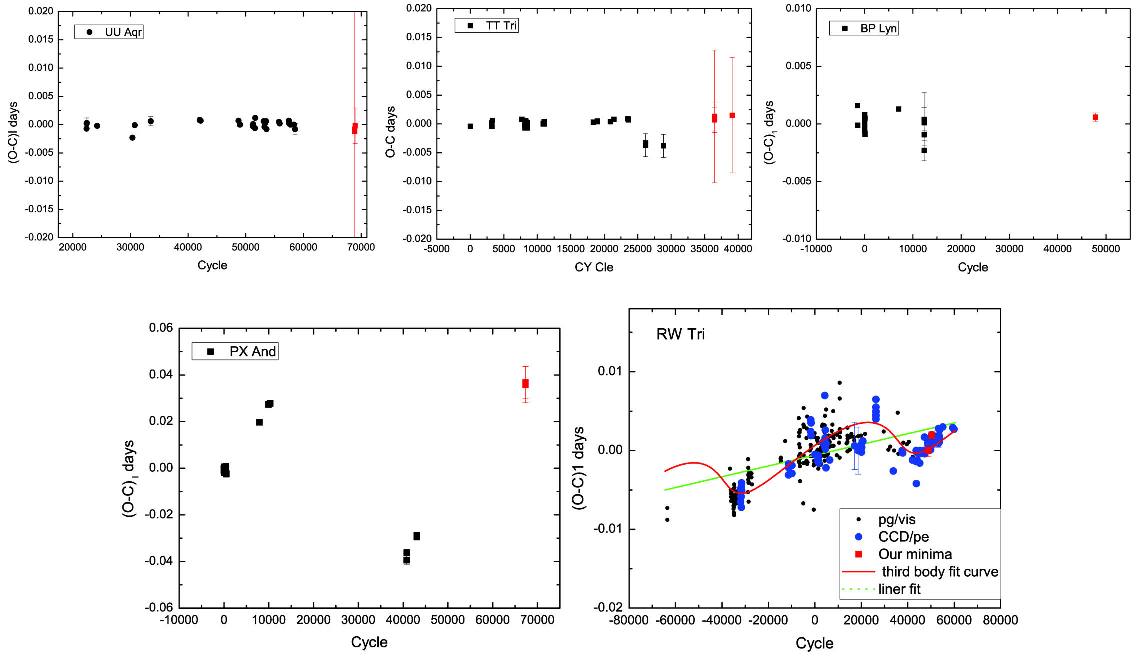

Fig. 5 Linear $(O-C)$ diagrams for five CVs: UU Aqr, TT Tri, PX And, BP Lyn and RW Tri. For RW Tri, the *red line* represents the fit of the third body in the subfigures.

We reduced CCD images by applying the IRAF package, including bias subtraction, flat-field division, cosmic ray removal and aperture photometry. We chose their comparison and check stars near our objects. We plotted the differential magnitudes (relative to the comparison stars) for these CVs in Figure 4, and listed them in Table 4, which includes the object name in the first column, the differential magnitude and observation filters in the 2nd-10th columns, and the telescope in the last column. For these light curves, we see strong flickering in part of the light curves outside eclipses. These are consistent with previous results (e.g., Baptista & Bortoletto 2008; Li et al. 1990; Warren et al. 2006; Grauer et al. 1994), which might be attributed to the stellar disk of accretion stream or stellar wind.

3.4 The Linear Ephemerides of Several CVs

By fitting our light curves with a polynomial function using a program, we obtained 13 new primary light minimum times and their uncertainties. We listed these new minima and corresponding uncertainties in Table 5. To obtain updated ephemerides and discuss orbital period variations, we collected all the available eclipse times from the literatures (e.g., Paschke & Brat 2006; Hellier & Robinson 1994; Atali et al. 2014) and listed them in Table 5. Subsequently, we obtained updated linear ephemerides for these CVs by applying least square fittings. The linear ephemerides are shown in Equation (1). All minima were weighted equally because there were no published errors for many of these minima, and they were all observed with a similar CCD method. We listed the relevant parameters in Table 5, which include star name in the first column, the minimum time in HJD and its uncertainty in the second and third columns, respectively, the type of minimum in the fourth columns (P means primary minima and S means secondary minima.), the observational method in the fifth column, cycle in the sixth column, the $O-C$ values of minimum times based on the updated linear ephemeris in the seventh column and references in the last column. To discuss the period variations, we plotted these values in Figure 5. As can be seen from Figure 5, there seem to be no obvious variations for UU Aqr, TT Tri and BP Lyn, but there is a variation for PX And. Because of the limited number of minima times, more observations of PX And are needed to determine its properties in the future.

$$\begin{aligned}
\text{UU Aqr : Min.I} &= \text{HJD } 2446347.2682(5) \\
&\quad + 0.163580417(9)^{\rm d}E \\
\text{PX And : Min.I} &= \text{HJD } 2449238.835(2) \\
&\quad + 0.14635277(6)^{\rm d}E \\
\text{TT Tri : Min.I} &= \text{HJD } 2452540.5325(3) \\
&\quad + 0.13963742(2)^{\rm d}E
\end{aligned}$$

Table 5 Parameters of Light Minimum Times and Linear Residuals for Five CVs

Star name	JD (Hel.)	Error	Minima	Method	Cycle	$(O-C)$	Reference
UU Aqr	50012.2867	0.0003	P	CCD	22405	–0.0007	[1]
UU Aqr	50016.0500		P	CCD	22428	0.0002	[2]
UU Aqr	50018.0130		P	CCD	22440	0.0003	[2]
UU Aqr	50311.4758	0.0009	P	CCD	24234	–0.0002	[1]
UU Aqr	51312.9130		P	CCD	30356	–0.0023	[2]
UU Aqr	51377.5295	0.0003	P	CCD	30751	–0.0001	[3]
UU Aqr	51833.2652	0.0003	P	CCD	33537	0.0006	[4]
UU Aqr	53222.5539	0.0008	P	CCD	42030	0.0008	[5]
UU Aqr	53250.3625	0.0005	P	CCD	42200	0.0007	[6]
UU Aqr	54323.4500		P	CCD	48760	0.0007	[2]
UU Aqr	54797.3430	0.003	P	CCD	51657	0.0012	[7]
...	...	...	...	...	...	...	...
UU Aqr	55893.3305		P	CCD	58357	0.0000	[2]
UU Aqr	55923.2650	0.0010	P	CCD	58540	–0.0008	[8]
UU Aqr	57614.5225	0.02951	P	CCD	68879	–0.0012	[9]
UU Aqr	57614.6865	0.07425	P	CCD	68880	–0.0008	[9]
UU Aqr	57631.5359	0.00314	P	CCD	68983	–0.0002	[9]
PX And	47781.8950		P	pe	–13	–0.0010	[10]
PX And	47782.7740		P	pe	–7	–0.0001	[10]
...	...	...	...	...	...	...	...
PX And	48942.7640		P	pe	7919	0.0197	[10]
PX And	49238.8378		P	pe	9942	0.0273	[11]
PX And	49297.6710		P	pe	10344	0.0278	[11]
PX And	53752.3519	0.0018	P	CCD	40783	–0.0394	[12]
PX And	53759.3799	0.0011	P	CCD	40831	–0.0362	[12]
PX And	54085.3082	0.0014	P	CCD	43058	–0.0294	[12]
PX And	54085.4551	0.0014	P	CCD	43059	–0.0289	[12]
PX And	57636.5576	0.00701	P	CCD	67323	0.0368	[9]
PX And	57636.7029	0.00773	P	CCD	67324	0.0358	[9]
TT Tri	54061.4633		P	ccd	10892	0.0000	[2]
TT Tri	54081.2922		P	ccd	11034	0.0004	[2]
TT Tri	56195.2590	0.002	P	ccd	26173	–0.0035	[13]
TT Tri	56195.3990	0.003	P	ccd	26174	–0.0032	[13]
TT Tri	56570.3250	0.002	P	ccd	28859	–0.0036	[13]
TT Tri	52540.5321		P	ccd	0	–0.0005	[14]
TT Tri	52989.3274		P	ccd	3214	0.0002	[14]
TT Tri	52990.3042		P	ccd	3221	–0.0005	[14]
TT Tri	52999.3816		P	ccd	3286	0.0005	[14]
TT Tri	54061.4634		P	ccd	10892	0.0001	[14]
TT Tri	54081.2921		P	ccd	11034	0.0003	[14]
TT Tri	54086.4584		P	ccd	11071	0.0001	[14]
TT Tri	53618.9531		P	ccd	7723	0.0008	[15]
TT Tri	53669.7801		P	ccd	8087	–0.0002	[15]
...	...	...	...	...	...	...	...
TT Tri	53728.7075		P	ccd	8509	0.0002	[15]
TT Tri	57633.6691	0.0115	P	ccd	36474	0.0016	[9]
TT Tri	57634.5063	0.0022	P	ccd	36480	0.0010	[9]
TT Tri	57634.6464	0.00642	P	ccd	36481	0.0014	[9]
TT Tri	57634.6464	0.010	P	ccd	39117	0.0015	[9]
BP Lyn	47658.75365		P	CCD	–1460	0.0016	[16]
BP Lyn	47659.66888		P	CCD	–1454	–0.0001	[16]
...	...	...	...	...	...	...	...
BP Lyn	48954.90924		P	CCD	7022	0.0013	[16]
BP Lyn	49765.5760	0.0009	P	CCD	12327	–0.0023	[17]
BP Lyn	49766.4943	0.0003	P	CCD	12333	–0.0009	[17]
BP Lyn	49766.6481	0.0013	P	CCD	12334	0.0001	[17]
BP Lyn	49767.5653	0.0023	P	CCD	12340	0.0004	[17]
BP Lyn	55188.28420	0.0004	P	CCD	47813	0.0006	[9]
...	...	...	...	...	...	...	...

Notes: [1] Safar & Zejda (2000); [2] Paschke & Brat (2006); [3] Safar & Zejda (2002); [4] Brát et al. (2007); [5] Zejda et al. (2006); [6] Hubscher & Walter (2007); [7] Paschke (2009); [8] Paschke (2012); [9] Our paper; [10] Hellier & Robinson (1994); [11] Li et al. (1990); [12] Kruspe et al. (2007); [13] Atali et al. (2014); [14] Rodríguez-Gil et al. (2007); [15] Warren et al. (2006); [16] Grauer et al. (1994); [17] Still (1996); [18] Walker (1963); [19] Surkova & Skatova (1969); [20] Warner (1973); [21]Polsgrove et al. (2006); [22] Diethelm (2003); [23] Diethelm (2004); [24] Krajci (2006); [25] Polsgrove et al. (2006); [26]Zejda et al. (2006); [27] Krajci (2007); [28] Diethelm (2010); [29] Diethelm (2011); [30] Hubscher & Lehmann (2012); [31] Diethelm (2012); [32] Diethelm (2013); [33] Hubscher (2017). The full list is at *http://www.raa-journal.org/docs/Supp/RAA4138Table5*.

Table 6 Parameters of the Third Body for RW Tri

Parameter	Value
A (d)	0.0031(2)
P_3 (yr)	47.6(0.4)
e	0.51(1)
T_P (HJD)	2452295.38(10)
$a_{12}\sin i$ (AU)	0.537(0.014)
K_{RV} (km s^{-1})	0.390(0.018)
$f(m)$ ($M_\odot$)	0.000068(6)
Residual	0.0046

$$\begin{aligned}\text{BP Lyn : Min.I} &= \text{HJD } 2447881.8583(3) \\ &\quad +0.15281253(2)^{\text{d}}E \\ \text{RW Tri : Min.I} &= \text{HJD } 2443512.6608(59) \\ &\quad +0.23188321(4)^{\text{d}}E \qquad (1)\end{aligned}$$

For RW Tri, there might be an oscillation in its $O-C$ diagram in Figure 5, which may be caused by the light-time effect due to the existence of a third body or magnetic cycle (e.g., Applegate 1992; Lanza et al. 1998). If the period oscillation is due to the light-time effect, then we can use a weighted nonlinear least-squares fitting (Yang et al. 2007) with the following equation describing the light time effect (Press et al. 1992)

$$\tau = \frac{a_{12}\sin i}{c}\Big(\frac{1-e^2}{1+e\cos\nu}\sin(\nu+\omega)+e\sin\omega\Big), (2)$$

where the semi-amplitude of the light-time effect is A = $a_{12}\sin i/c, a_{12}$ is the semiaxis of the eclipsing - pair orbiting around the common center of mass with the third body and c is the speed of light. Orbital parameters for the third body are ν, e, ω and i, which correspond to the true anomaly, eccentricity, longitude of periastron and inclination, respectively. Here M_1, M_2 and M_3 are the masses of the primary, secondary and third body, respectively. We can calculate the mass of the third component with the equation

$$f(m) = \frac{4\pi^2}{GT^2}\times({a'}_{12}\sin i')^3 = \frac{(M_3\sin i_3')^3}{(M_1+M_2+M_3)^2}.$$

The parameters of the third body and the fit residual for RW Tri are listed in Table 6. The mass of the third body depends on the orbital inclination. We used M_1 as 0.7 $M_\odot$, M_2 as 0.6 $M_\odot$ and orbital inclination of 75 degrees for RW Tri (Rutten et al. 1992), and obtained the third mass $M_{3,\min}$ to be 0.052 $M_\odot$ when i'=75°. The mass of the third body is below the stable hydrogen burning limit of about 0.072 $M_\odot$ and thus it might be a brown dwarf.

4 CONCLUSIONS

The analyses of CVs observed in the stellar spectral survey LAMOST DR3 are summarized as follows:

(1) We cross-matched the CV catalog with the LAMOST stellar survey (DR3) and found new CV candidates from LAMOST DR3. We also obtained their EWs in several Balmer lines and two HeI lines.
(2) We identified 74 stellar spectra for 48 known CVs, and three stellar spectra for three new CV candidates. We also found 33 objects with repeated observations and 30 stars showing spectral variability in the Hα line.
(3) We made photometric follow-up CCD observations for five CVs (UU Aqr, TT Tri, PX And, BP Lyn and RW Tri) and obtained nine new light curves. We identified 13 new light minima and revised their linear ephemerides. For RW Tri, there is a possible oscillation with an amplitude of 0.0031(2) days and a period of 47.6 ± 0.4 years, which might be caused by a third body or magnetic activity cycle.

Acknowledgements This work is supported by the Joint Research Fund in Astronomy (U1631236 and U1431114) under cooperative agreement between the National Natural Science Foundation of China (NSFC, Nos. 11263001 and 11563002) and Chinese Academy of Sciences (CAS). The Guo Shou Jing Telescope is a National Major Scientific Project built by CAS. Funding for the project has been provided by the National Development and Reform Commission. LAMOST is operated and managed by NAOC, CAS. We would also like to thank Dr. Frank Levinson for his generous financial support which enabled Butler University to join the SARA telescope consortium. We acknowledge support from the staff at the Xinglong 85-cm telescope and Lijiang 2.4-m telescopes. Funding for the 2.4-m telescope has been provided by CAS and the People's Government of Yunnan Province. This work was partially supported by the Open Project Program of the Key Laboratory of Optical Astronomy, NAOC, CAS. This work was also supported by the Natural Science Foundation for Young Scientists (Grant No. 2014298) from the Office of Education of Guizhou Province.

References

Africano, J. L., Nather, R. E., Patterson, J., Robinson, E. L., & Warner, B. 1978, PASP, 90, 568
Applegate, J. H. 1992, ApJ, 385, 621

Atali, H. B., Alis, S., Yelkenci, K., et al. 2014, Information Bulletin on Variable Stars, 6102
Austin, S. J., Robertson, J. W., de Souza, T. R., Tycner, C., & Honeycutt, R. K. 2011, AJ, 141, 124
Baptista, R., & Bortoletto, A. 2008, ApJ, 676, 1240
Baptista, R., Silveira, C., Steiner, J. E., & Horne, K. 2000, MNRAS, 314, 713
Baptista, R., Steiner, J. E., & Cieslinski, D. 1994, ApJ, 433, 332
Bianchini, A. 1980, MNRAS, 192, 127
Brát, L., Zejda, M., & Svoboda, P. 2007, Open European Journal on Variable Stars, 74, 1
Breedt, E., Gänsicke, B. T., Drake, A. J., et al. 2014, MNRAS, 443, 3174
Casares, J., Martinez-Pais, I. G., Marsh, T. R., Charles, P. A., & Lazaro, C. 1996, MNRAS, 278, 219
Chen, L., Hou, J.-L., Yu, J.-C., et al. 2012, RAA (Research in Astronomy and Astrophysics), 12, 805
Cui, X.-Q., Zhao, Y.-H., Chu, Y.-Q., et al. 2012, RAA (Research in Astronomy and Astrophysics), 12, 1197
Dai, Z., Qian, S., & Li, L. 2013, ApJ, 774, 153
Deng, L.-C., Newberg, H. J., Liu, C., et al. 2012, RAA (Research in Astronomy and Astrophysics), 12, 735
Dhillon, V. S., Jones, D. H. P., Marsh, T. R., & Smith, R. C. 1992, MNRAS, 258, 225
Diethelm, R. 2003, Information Bulletin on Variable Stars, 5438
Diethelm, R. 2004, Information Bulletin on Variable Stars, 5543
Diethelm, R. 2010, Information Bulletin on Variable Stars, 5920
Diethelm, R. 2011, Information Bulletin on Variable Stars, 5960
Diethelm, R. 2012, Information Bulletin on Variable Stars, 6011
Diethelm, R. 2013, Information Bulletin on Variable Stars, 6042
Dillon, M., Gänsicke, B. T., Aungwerojwit, A., et al. 2008, MNRAS, 386, 1568
Dobrotka, A., Mineshige, S., & Casares, J. 2012, MNRAS, 420, 2467
Downes, R. A., Webbink, R. F., Shara, M. M., et al. 2001, PASP, 113, 764
Downes, R., Hoard, D. W., Szkody, P., & Wachter, S. 1995, AJ, 110, 1824
Drake, A. J., Gänsicke, B. T., Djorgovski, S. G., et al. 2014, MNRAS, 441, 1186
Fan, Y.-F., Bai, J.-M., Zhang, J.-J., et al. 2015, RAA (Research in Astronomy and Astrophysics), 15, 918
Gänsicke, B. T., Marsh, T. R., Edge, A., et al. 2005, MNRAS, 361, 141
Giovannelli, F. 2008, Chinese Journal of Astronomy and Astrophysics Supplement, 8, 237
Girven, J., Gänsicke, B. T., Steeghs, D., & Koester, D. 2011, MNRAS, 417, 1210
Grauer, A. D., Ringwald, F. A., Wegner, G., et al. 1994, AJ, 108, 214
Green, R. F., Ferguson, D. H., Liebert, J., & Schmidt, M. 1982, PASP, 94, 560
Hellier, C., & Robinson, E. L. 1994, ApJ, 431, L107
Hoard, D. W., & Szkody, P. 1996, ApJ, 470, 1052
Honeycutt, R. K., Robertson, J. W., & Turner, G. W. 1998, AJ, 115, 2527
Hubscher, J. 2017, Information Bulletin on Variable Stars, 6196
Hubscher, J., & Lehmann, P. B. 2012, Information Bulletin on Variable Stars, 6026
Hubscher, J., & Walter, F. 2007, Information Bulletin on Variable Stars, 5761
Isogai, M., Arai, A., Yonehara, A., et al. 2015, PASJ, 67, 7
Jiang, B., Luo, A., Zhao, Y., & Wei, P. 2013, MNRAS, 430, 986
Kaitchuck, R. H., Schlegel, E. M., & Honeycutt, R. K. 1983, ApJ, 267, 239
Kato, T., Imada, A., Uemura, M., et al. 2009, PASJ, 61, S395
Keel, W. C., Oswalt, T., Mack, P., et al. 2017, PASP, 129, 015002
Khruzina, T., Katysheva, N., Golysheva, P., & Shugarov, S. 2015, in EAS Publications Series, 71, EAS Publications Series, 149
Kjurkchieva, D., Marchev, D., Khruzina, T., & Djurašević, G. 2006, Ap&SS, 306, 217
Krajci, T. 2006, Information Bulletin on Variable Stars, 5690
Krajci, T. 2007, Information Bulletin on Variable Stars, 5806
Kruspe, R., Schuh, S., & Traulsen, I. 2007, Information Bulletin on Variable Stars, 5796
Lanza, A. F., Rodono, M., & Rosner, R. 1998, MNRAS, 296, 893
Lazaro, C., Martinez-Pais, I. G., Arevalo, M. J., & Solheim, J. E. 1991, AJ, 101, 196
Li, Y., Jiang, Z.-j., Chkn, J.-s., & Wei, M.-z. 1990, Chinese Astronomy and Astrophysics, 14, 359
Liu, W., & Hu, J. Y. 2000, ApJS, 128, 387
Liu, W., Hu, J. Y., Zhu, X. H., & Li, Z. Y. 1999, ApJS, 122, 243
Liu, X.-W., Zhao, G., & Hou, J.-L. 2015, RAA (Research in Astronomy and Astrophysics), 15, 1089
Luo, A.-L., Zhang, H.-T., Zhao, Y.-H., et al. 2012, RAA (Research in Astronomy and Astrophysics), 12, 1243
Luo, A.-L., Zhao, Y.-H., Zhao, G., et al. 2015, RAA (Research in Astronomy and Astrophysics), 15, 1095
Matthews, J. H., Knigge, C., Long, K. S., Sim, S. A., & Higginbottom, N. 2015, MNRAS, 450, 3331
Paschke, A. 2009, Open European Journal on Variable Stars, 116, 1
Paschke, A. 2012, Open European Journal on Variable Stars,

147, 1
Paschke, A., & Brat L., 2006, OEJV, 23, 13
Patterson, J., Thorstensen, J. R., Vanmunster, T., et al. 2004, PASP, 116, 516
Patterson, J., Kemp, J., Harvey, D. A., et al. 2005, PASP, 117, 1204
Patterson, J., Thorstensen, J. R., Sheets, H. A., et al. 2011, PASP, 123, 130
Polsgrove, D. E., Wetterer, C. J., Bloomer, R. H., & Newton, J. D. 2006, Information Bulletin on Variable Stars, 5710
Poole, T., Mason, K. O., Ramsay, G., Drew, J. E., & Smith, R. C. 2003, MNRAS, 340, 499
Press, W. H., Teukolsky, S. A., Vetterling, W. T., & Flannery, B. P. 1992, Numerical recipes in FORTRAN. The Art of Scientific Computing (Cambridge: Cambridge University Press, 2nd ed.)
Qian, S.-B., Liao, W.-P., Zhu, L.-Y., et al. 2010, MNRAS, 401, L34
Ringwald, F. A., Chase, D. W., & Reynolds, D. S. 2005, PASP, 117, 1223
Rodríguez-Gil, P., Gänsicke, B. T., Hagen, H.-J., et al. 2007, MNRAS, 377, 1747
Romano, G. . 1978, Information Bulletin on Variable Stars, 1421
Rutten, R. G. M., & Dhillon, V. S. 1992, A&A, 253, 139
Rutten, R. G. M., van Paradijs, J., & Tinbergen, J. 1992, A&A, 260, 213
Safar, J., & Zejda, M. 2000, Information Bulletin on Variable Stars, 4887
Safar, J., & Zejda, M. 2002, Information Bulletin on Variable Stars, 5263
Sheets, H. A., Thorstensen, J. R., Peters, C. J., Kapusta, A. B., & Taylor, C. J. 2007, PASP, 119, 494
Sion, E. M. 1986, PASP, 98, 821
Skidmore, W., Horne, K., Pearson, K., et al. 2004, in Revista Mexicana de Astronomia y Astrofisica Conference Series, 20, ed. G. Tovmassian & E. Sion, 155
Skrutskie, M. F., Cutri, R. M., Stiening, R., et al. 2006, AJ, 131, 1163
Smak, J. 1995, Acta Astronomica, 45, 259
Southworth, J., Gänsicke, B. T., Marsh, T. R., et al. 2006, MNRAS, 373, 687
Southworth, J., Tappert, C., Gänsicke, B. T., & Copperwheat, C. M. 2015, A&A, 573, A61
Stanishev, V., Kraicheva, Z., Boffin, H. M. J., & Genkov, V. 2002, A&A, 394, 625
Still, M. D. 1996, MNRAS, 282, 943
Still, M. D., Dhillon, V. S., & Jones, D. H. P. 1995, MNRAS, 273, 863
Surkova, L. P., & Skatova, N. V. 1969, Information Bulletin on Variable Stars, 394
Szkody, P. 2015, Acta Polytechnica CTU Proceedings, 2, 55
Szkody P., Everett M. E., Howell S. B., et al., 2014, AJ, 148, 63
Szkody, P., & Howell, S. B. 1992, ApJS, 78, 537
Szkody, P., Anderson, S. F., Agüeros, M., et al. 2002, AJ, 123, 430
Szkody, P., Fraser, O., Silvestri, N., et al. 2003, AJ, 126, 1499
Szkody, P., Henden, A., Fraser, O., et al. 2004, AJ, 128, 1882
Szkody, P., Henden, A., Fraser, O. J., et al. 2005, AJ, 129, 2386
Szkody, P., Henden, A., Agüeros, M., et al. 2006, AJ, 131, 973
Szkody, P., Henden, A., Mannikko, L., et al. 2007, AJ, 134, 185
Szkody, P., Anderson, S. F., Hayden, M., et al. 2009, AJ, 137, 4011
Szkody, P., Anderson, S. F., Brooks, K., et al. 2011, AJ, 142, 181
Thorstensen, J. R. 2000, PASP, 112, 1269
Thorstensen, J. R., Alper, E. H., & Weil, K. E. 2016, AJ, 152, 226
Thorstensen, J. R., Ringwald, F. A., Wade, R. A., Schmidt, G. D., & Norsworthy, J. E. 1991, AJ, 102, 272
Thorstensen, J. R., Taylor, C. J., & Kemp, J. 1998, PASP, 110, 1405
Unda-Sanzana, E., Marsh, T. R., & Morales-Rueda, L. 2006, MNRAS, 369, 805
Walker, M. F. 1963, ApJ, 137, 485
Wang, S.-G., Su, D.-Q., Chu, Y.-Q., Cui, X., & Wang, Y.-N. 1996, Appl. Opt., 35, 5155
Warner, B. 1973, Information Bulletin on Variable Stars, 852
Warner, B. 1995, Cataclysmic Variable Stars in: Cambridge Astrophysics Series, 28
Warren, S. R., Shafter, A. W., & Reed, J. K. 2006, PASP, 118, 1373
Wegner, G., & McMahan, R. K. 1985, AJ, 90, 1511
Wei, P., Luo, A., Li, Y., et al. 2013, MNRAS, 431, 1800
Wei, P., Luo, A., Li, Y., et al. 2014, AJ, 147, 101
Witham, A. R., Knigge, C., Aungwerojwit, A., et al. 2007, MNRAS, 382, 1158
Woudt, P. A., Warner, B., de Budé, D., et al. 2012, MNRAS, 421, 2414
Yang, Y.-G., Dai, J.-M., Yin, X.-G., & Xiang, F.-Y. 2007, AJ, 134, 179
York, D. G., Adelman, J., Anderson, Jr., J. E., et al. 2000, AJ, 120, 1579
Zejda, M., Mikulasek, Z., & Wolf, M. 2006, Information Bulletin on Variable Stars, 5741
Zhang, L.-Y., & Gu, S.-H. 2008, A&A, 487, 709
Zhang, L.-Y., Yue, Q., Lu, H.-P., et al. 2017, RAA (Research in Astronomy and Astrophysics), 17, 105
Zhang, L., Pi, Q., Han, X. L., et al. 2016, New Astron., 44, 66
Zhang, L., Lu, H., Han, X. L., et al. 2018, New Astron., 61, 36
Zhou, A.-Y., Jiang, X.-J., Zhang, Y.-P., & Wei, J.-Y. 2009, RAA (Research in Astronomy and Astrophysics), 9, 349
Zwitter, T., & Munari, U. 1994, A&AS, 107, 503